NASA Technical Memorandum 1999–206892, Volume 5

SeaWiFS Postlaunch Technical Report Series

Stanford B. Hooker, Editor
NASA Goddard Space Flight Center
Greenbelt, Maryland

Elaine R. Firestone, Senior Technical Editor
SAIC General Sciences Corporation
Beltsville, Maryland

Volume 5, The SeaWiFS Solar Radiation-Based Calibration and the Transfer-to-Orbit Experiment

Robert A. Barnes and Robert E. Eplee, Jr.
SAIC General Sciences Corporation
Beltsville, Maryland

Stuart F. Biggar, Kurtis J. Thome, Edward F. Zalewski, and Philip N. Slater
University of Arizona
Tucson, Arizona

Alan W. Holmes
Santa Barbara Instrument Group
Santa Barbara, California

Abstract

The solar radiation-based calibration (SRBC) of the Sea-viewing Wide Field-of-view Sensor (SeaWiFS) was performed on 1 November 1993. Measurements were made outdoors in the courtyard of the instrument manufacturer. SeaWiFS viewed the solar irradiance reflected from the sensor's diffuser in the same manner as viewed on orbit. The calibration included measurements using a solar radiometer designed to determine the transmittances of principal atmospheric constituents. The primary uncertainties in the outdoor measurements are the transmission of the atmosphere and the reflectance of the diffuser. Their combined uncertainty is about 5 or 6%. The SRBC also requires knowledge of the extraterrestrial solar spectrum. Four solar models are used. When averaged over the responses of the SeaWiFS bands, the irradiance models agree at the 3.6% level, with the greatest difference for SeaWiFS band 8. The calibration coefficients from the SRBC are lower than those from the laboratory calibration of the instrument in 1997. For a representative solar model, the ratios of the SRBC coefficients to laboratory values average 0.962 with a standard deviation of 0.012. The greatest relative difference is 0.946 for band 8. These values are within the estimated uncertainties of the calibration measurements. For the transfer-to-orbit experiment, the measurements in the manufacturer's courtyard are used to predict the digital counts from the instrument on its first day on orbit (1 August 1997). This experiment requires an estimate of the relative change in the diffuser response for the period between the launch of the instrument and its first solar measurements on orbit (9 September 1997). In relative terms, the counts from the instrument on its first day on orbit averaged 1.3% higher than predicted, with a standard deviation of 1.2% and a greatest difference of 2.4% for band 7. The estimated uncertainty for the transfer-to-orbit experiment is about 3 or 4%.

1. INTRODUCTION

Integrating sphere sources are commonly used for the preflight calibration of sensors in the solar reflected spectral range. They have the advantage of providing a full aperture, full field of view, end-to-end calibration at several different points over the dynamic range of the instrument. Integrating sphere sources, however, have several disadvantages related to the lamps and to the reflective coatings of the spheres.

Tungsten quartz halogen lamps, operated at a color temperature of about 3,000 K, are usually used to illuminate the sphere interior. The output of these lamps peaks at about 1 μm and falls off rapidly at shorter wavelengths. As a result, it is difficult to match the radiance level of solar radiation reflected from the atmosphere and surface of the Earth at short wavelengths using an integrating sphere source. Also, the rapid fall off of the spectral radiance from the sphere makes it both difficult to measure and to accurately calibrate the sensor's short wavelength spectral bands. Furthermore, measurements made by the sensor on orbit are of reflected solar radiation which contains Fraunhofer lines, whereas lamps do not include these sharp spectral features. For sensors with narrow spectral bandpasses, that is, less than 10 nm, the presence of a Fraunhofer line within a bandpass can change the band-averaged response of the sensor by several percent with respect to its integrating sphere source calibration (Flittner and Slater 1991).

The interior of a large sphere source is usually coated with barium sulfate ($BaSO_4$) paint. The spectral reflectance of the paint is reasonably flat in the visible and the near infrared, but exhibits spectral structure in the short-wave infrared that is difficult to account for accurately in a calibration. Integrating sphere sources also have some instabilities associated with them. There are several causes, including the instability of the power supplies and the warm-up time required for the lamps to become stable. In addition, there are uncertainties associated with the calibration of the irradiance standard used to calibrate the output radiance of the sphere, the transfer of the lamp scale to the sphere output, and the aging of the sphere lamps and coating. The uncertainties in the irradiance standard are a function of wavelength, being approximately $\pm 1\%$ in the visible, but greater than $\pm 2\%$ in the short-wave infrared. (All uncertainties given in this document are one standard deviation, or 1σ.) When all of the sources of uncertainty for measurements of integrating sphere sources are considered, it is obvious that to achieve an uncertainty as low as, say, $\pm 3\%$ for the sphere output, is very difficult, time consuming, and costly. Furthermore, in practice, a calibration using an integrating sphere source could be inaccurate for spectral bands of the sensor that fall over strong Fraunhofer lines.

The best form of onboard calibration is provided by a solar diffuser that is end-to-end, full aperture and full field, and because it is illuminated by the sun, has the appropriate spectral distribution and radiance levels at all wavelengths. One of the main shortcomings of solar diffusers, however, has been that no method has been found to calibrate the sensor preflight using the solar diffuser without using the aforementioned tungsten lamps. The assumption has to be made, therefore, that the in-flight calibration of

the sensor via the solar diffuser is not subject to systematic errors. This assumption implies that the reflectance of the diffuser and the irradiance on the diffuser are both accurately known. Without the use of a ratio-taking radiometer (Slater and Palmer 1991), or an alternative solar diffuser monitor (Pagano and Durham 1993, and Bruegge et al. 1993), assumptions must be made concerning the absence of stray light and contamination of the diffuser. In any case, the results of an onboard diffuser-based calibration can only be approximately related to a preflight integrating sphere source calibration. This is partly because of the reasons given earlier, and partly because of the uncertainty in the current scientific knowledge of the exoatmospheric spectral irradiance.

This report describes an attempt to use measurements of the sun to quantify changes in the prelaunch calibration of a satellite instrument during its insertion into orbit. For this experiment, the diffuser is illuminated by the sun while on the ground before launch, and then on orbit after launch. An attempt at a preflight solar radiation-based calibration (SRBC) of a sensor and diffuser system is also described, which was conducted using the same illumination and viewing geometry used during in-flight calibration.

The preflight solar-based calibration can be directly compared to the preflight integrating sphere absolute radiance calibration, providing a desirable link between in-flight solar-based calibration and the preflight sphere-based calibration; the link is to national laboratory standards in physical units. With respect to national standards, it is worth emphasizing that, although knowledge of the sun's absolute radiance in physical units is uncertain, the sun's *output* is the same anywhere on Earth, while the irradiance and radiance scales between different national standards laboratories vary.

There are different risks and disadvantages associated with the solar-based method of calibrating a sensor. First and foremost is the risk to the sensor associated with the move to an appropriate site outside. There is also a chance of contamination of the optics when actually doing the experiment. Clear sky conditions are required, and a very low aerosol loading is best. Accurate atmospheric transmittance measurements are required. High accuracy solar exoatmospheric spectral data are needed to provide an accurate comparison with national laboratory standards. The currently available solar data are not sufficiently accurate, nor of high enough spectral resolution, for such a comparison.

The calibration procedure necessitates illuminating the diffuser on the flight sensor with direct solar irradiation. Heath (pers. comm.) described a similar procedure, not for sensor calibration purposes, but to provide a measure of the relative ozone columnar concentration from the various Solar Backscatter Ultraviolet (SBUV) instrument spectral bands.

In order to calibrate SeaWiFS via the diffuser, the sensor and electronics had to be taken outside. (In the case of the SBUV instrument, the laboratory roof was opened.) The possibility of taking a flight unit sensor was not anticipated by the authors until the first SeaWiFS Science Team meeting in January 1993. During a presentation by the instrument manufacturer, Raytheon Santa Barbara Research Center (SBRC)†, A. Holmes, remarked that this was done to check that the appropriate gain settings had been selected for diffuser and lunar viewing. This prompted P. Slater to propose to the Science Team that a solar-based preflight calibration be attempted. Such an approach was approved by the Science Team and the project managers from the National Aeronautic and Space Administration (NASA) Goddard Space Flight Center (GSFC) and SBRC. The hour-long calibration, described here, was conducted on 1 November 1993.

2. SRBC

For the SRBC, SeaWiFS viewed the radiance from its diffuser. When combined with counts from the instrument during the diffuser measurements, calibration coefficients for the SeaWiFS bands were determined.

2.1 Concept

The concept is simple. An attempt is made to duplicate, on the ground, the solar illumination conditions seen by the sensor on orbit. The simulation requires just the direct solar beam, and it must illuminate the diffuser at the incidence angles used during in-flight calibrations. The requirement for just the direct solar beam is a difficult one. At the ground level, there is substantial scattering of the solar flux by molecules in the atmosphere, as well as by the aerosols distributed in the lower part of the atmosphere. This scattering is strongly wavelength dependent and causes a variable amount of diffuse light that can illuminate the diffuser from angles other than the solar incidence angle.

The atmosphere also attenuates the direct beam of solar flux, as compared to the beam at the top of the atmosphere. The simulation must compensate, therefore, for the lower-than-unity atmospheric transmittance. Part of the transmittance loss is caused by absorption by gases such as ozone, oxygen, and water vapor. Another cause of lower transmittance is the loss due to scattering of light out of the direct beam into the diffuse field. In order to make the calibration, corrections are made both for the atmospheric transmittance and for the diffuse light that illuminates the diffuser. These corrections are discussed in Sects. 2.3.3 and 2.4, respectively.

† The Raytheon Santa Barbara Research Center was formerly known as Hughes Santa Barbara Remote Sensing, a subsidiary of Hughes Aircraft.

2.2 Reflectance Equations

There are several factors in determining the radiance from the SeaWiFS diffuser. Central among these factors is the reflectance function for the diffuser. This function describes the ratio of the scattered radiance from the diffuser to the incident irradiance. It is called the bidirectional reflectance distribution function (BRDF), and it has units of inverse steradians, i.e., per unit solid angle.

2.2.1 BRDF

At a single wavelength, the basic equation for the effect of the diffuser on the incident sunlight is the ratio of the scattered to the incident radiation. The scattered radiation is measured as radiance (watts per unit area per unit solid angle), and the incident radiation is measured as irradiance (watts per unit area). The BRDF is defined as

$$B(\lambda) \;=\; \frac{\int L(\lambda)\,\theta_S\,\cos(\theta_S)\,dA_S\,d\Omega}{\int E(\lambda)\,\theta_I\,\cos(\theta_I)\,dA_I}, \qquad (1)$$

where θ_I is the angle of incidence and θ_S is the angle of view (that is, the scattering angle). Both angles are given with respect to the normal to the scattering surface. In (1), $L(\lambda)\theta_S$ is the scattered radiance at wavelength λ, $E(\lambda)\theta_I$ is the incident irradiance, and $B(\lambda)$ is the BRDF. The terms dA_S and dA_I are differential areas on the surface of the scattering surface, and $d\Omega$ is a differential of solid angle. The terms $\cos(\theta_I)$ and $\cos(\theta_S)$ are corrections to the incident and scattered flux when they are not normal to the surface. The word "bidirectional" refers to measurements of the reflection ratio made at all angles of incidence (that is, at all zenith and azimuthal angles over an entire hemisphere) and all zenith and azimuthal angles into which the radiation is scattered. For the SeaWiFS diffuser, the solar irradiance is limited to a small set of angles of incidence. The scattered radiation is measured in only one direction, that of the view of the telescope. In this case, θ_S is constant and θ_I varies slightly, and because the area irradiated and the area viewed are the same, the BRDF equation simplifies to

$$B(\lambda) \;=\; \frac{\pi L(\lambda)}{E(\lambda)\cos(\theta_I)}. \qquad (2)$$

In (2), the value of π comes from the integration over the range of zenith and azimuthal angles.

The characterization of the SeaWiFS diffuser is based on (2). The end-to-end, system level characterization by SBRC connected the diffuser response to that of the instrument for views of the Earth at instrument nadir. For these measurements, the diffuser was illuminated with a source having an angular subtense similar to that of the sun. The illumination source was a 1,000 W FEL lamp placed about 300 cm from the instrument. Determining the reflectance required two measurements. For the first measurement, the light from the lamp was measured using the SeaWiFS diffuser. This measurement was made with the lamp aligned with the diffuser's input aperture, so that the lamp's irradiance was normal to that aperture. For this measurement, the output from SeaWiFS gave the radiance scattered from the SeaWiFS diffuser.

For the second measurement, the instrument was rotated to measure the reflected light from a second diffuser as if the instrument were viewing the Earth. In the second measurement, the light from the lamp was reflected off a pressed halon diffuser with known reflectance and with nearly Lambertian response (Barnes and Eplee 1996). For the second measurement, the irradiance from the FEL lamp was normal to the surface of the halon diffuser, and SeaWiFS measured the scattered radiance at an angle of approximately 45° from normal. The ratio of the two measurements (SeaWiFS diffuser to halon diffuser) was used to calculate the reflectance of the instrument diffuser.

For the laboratory characterization of the SeaWiFS diffuser, the scattered radiance from the onboard diffuser included instrumental factors, such as, possible scattered light within the diffuser cavity, and geometric factors, including the incidence angle of the irradiance from the FEL lamp on the SeaWiFS diffuser. For the measurement of the halon diffuser, the incidence angle of the irradiance was zero, and the factor of π was included in its reflectance ($0.99/\pi$). These factors allow an additional simplification of the BRDF equation for the SeaWiFS diffuser,

$$F(\lambda) \;=\; \frac{L(\lambda)}{E(\lambda)}, \qquad (3)$$

where $F(\lambda)$ is the BRDF of the SeaWiFS diffuser at wavelength λ. The change in the BRDF symbol from (2) to (3) is a reminder of this additional simplification.

For the SRBC, the sun is the source of irradiance. The solar irradiances used here come from the tabulated results of models. These models are measurement based, and their irradiances are given for a standard Earth–sun distance of 1 AU, which is approximately 1.5×10^8 km. Figure 1 shows the values from Wehrli (1985) interpolated to 1 nm intervals from 380–1,150 nm; the solar irradiances from `MODTRAN` (Berk et al. 1989); the values from the `6S` code (Vermote et al. 1997); and those from Thuillier et al. (1998) in panels a, b, c, and d, respectively. The irradiance from the sun per unit solid angle is considered to be constant. The closer the Earth is to the sun, the greater the solid angle it (and the instrument diffuser) subtends. This is the reason for the inverse square law effect,

$$E(\lambda) \;=\; \frac{E(S,\lambda)}{D^2}, \qquad (4)$$

where $E(S,\lambda)$ is the solar irradiance at 1 AU and D is the Earth–sun distance (in astronomical units) at the time of

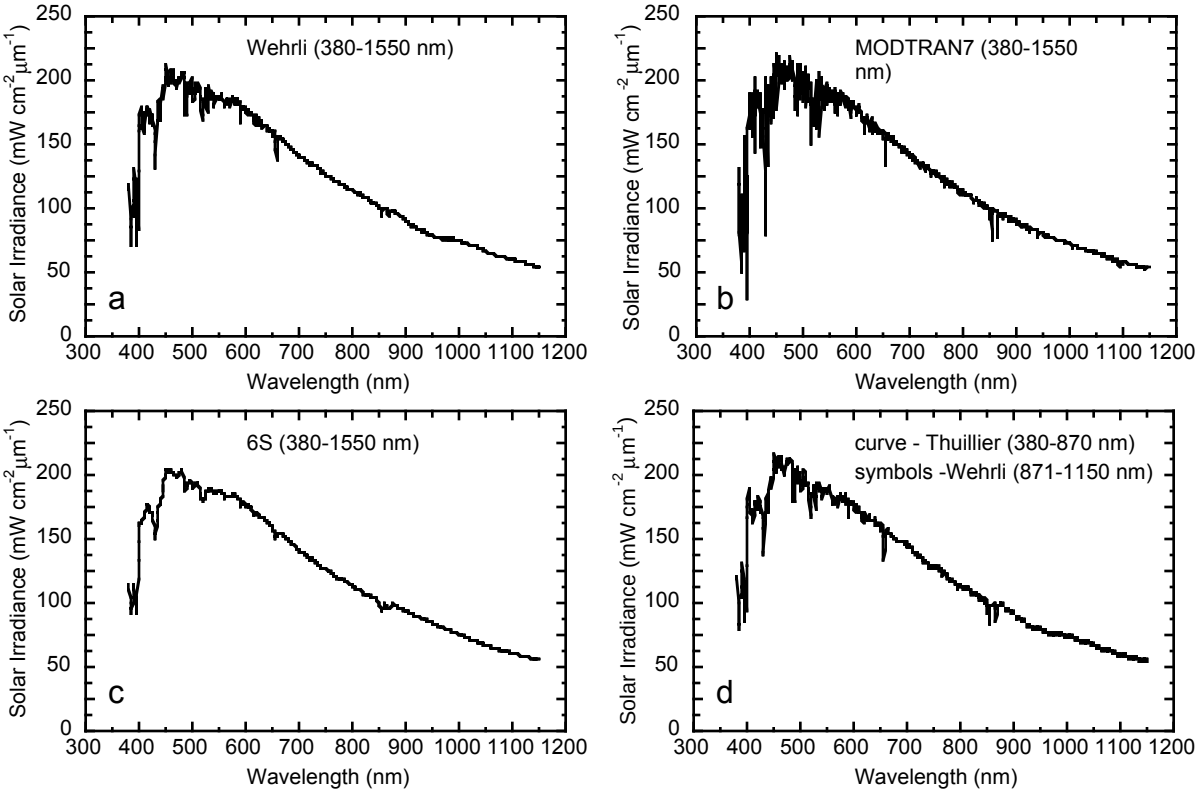

Fig. 1. Solar irradiance values used in these calculations. The irradiances are given for an Earth–sun distance of 1 AU, with units of $\mathrm{mW\,cm^{-2}\,\mu m^{-1}}$: **a)** the Wehrli model, and **b)** the `MODTRAN` model, **c)** the `6S` model, and **d)** values from the measurements of Thuillier et al. (1998). The measured values cover the range from 380–880 nm. These data are extended to 1,150 nm using the values from the model of Wehrli (1985).

the measurement. The irradiance for a direct view of the sun in space is given in (4).

For an instrument that measures at wavelength λ, there is a relationship between the output of the instrument and the input spectral radiance, which is defined here as

$$L(\lambda) \;=\; (DN - DN_0)\, k_2(g), \tag{5}$$

where DN is the output from the instrument in counts (digital numbers) when it views $L(\lambda)$; DN_0 is the output when the instrument measures zero radiance (the zero offset), and $k_2(g)$ is the calibration coefficient for the instrument with units of $\mathrm{mW\,cm^{-2}\,sr^{-1}\,\mu m^{-1}\,count^{-1}}$ (Barnes et al. 1994, Barnes and Eplee 1997, and Johnson et al. 1999). These calibration coefficients are based on measurements by the instrument of an integrating sphere in the laboratory. The gain factor, g, is a multiplier (dimensionless) within the instrument's electronics that allows for a reasonable output from the instrument for brighter (gain less than 1) and dimmer (gain greater than 1) radiance sources. The coefficients from the 1997 calibration of SeaWiFS are given in Sect. 2.5.1. They are the values for $k_2(g)$ for each band and gain. In an identical manner, the coefficients for the 1993 calibration of SeaWiFS are given in Sect. 2.5.2. The solar radiation-based calibration also provides values of $k_2(g)$, which can be compared with those from the laboratory.

It is possible to combine (3), (4), and (5) and solve for the instrument output in counts using

$$\begin{aligned}(DN - DN_0) \;&=\; \frac{L(\lambda)}{k_2(g)} \\ &=\; \frac{E(\lambda)\, F(\lambda)}{k_2(g)}\end{aligned}. \tag{6}$$

Implicit in this equation is the assumption that the instrument's response occurs at wavelength λ, and is zero at other wavelengths, that is, the response of the instrument is monochromatic. Another name for this type of response is a Dirac delta function, however, this is not the case for real instruments, such as SeaWiFS, which respond to radiance over a range of wavelengths.

2.2.2 Spectral Response

For real instruments, the spectral response can be defined in several ways. One definition is

$$\int_{\lambda_1}^{\lambda_2} R(\lambda)\, d\lambda \;=\; 1, \tag{7}$$

where $R(\lambda)$ is the spectral response at wavelength λ, and λ_1 and λ_2 are the lower and upper limits of integration, respectively. The integration limits mark the wavelength region within which the instrument has a significant (nonzero) response. The normalization of the integral to unity is a reminder that (7) includes all of the response of the instrument, as in Fig. 1 of Gordon (1995). This definition of spectral response gives values that are normalized to a constant; thus, the values from this definition are relative spectral responses.

It is also possible to normalize the spectral response to a maximum value of unity. This provides a second definition, also a relative spectral response. For this definition, the integral of the relative spectral response gives the bandwidth of the measuring band, that is, the equivalent width of a square wave relative spectral response (RSR) with a maximum value of unity. The bandwidths for the SeaWiFS bands are given in Barnes (1996).

A third definition of the spectral response is based on the optical and electrical characteristics of the instrument from its input aperture to the output of the photodiodes (Barnes et al. 1994). The photodiodes convert radiant flux (photons) into electrical current (electrons). In this definition, the spectral response is the output of the photodiode to a source with a constant spectral radiance of unity. There is a *hidden* $L(\lambda)$ in this definition, where

$$R(\lambda) \;=\; \xi(\lambda)\, Q(\lambda). \tag{8}$$

For SeaWiFS, $\xi(\lambda)$ is the combined reflecting–transmitting efficiency of the optical components between the instrument's entrance aperture and the photodiode (dimensionless), and $Q(\lambda)$ is the conversion efficiency of the photodiode, with units of electrical current per unit of radiance at each wavelength λ (see Barnes et al. 1994 for details). For SeaWiFS, these units are $\mathrm{pA\,mW^{-1}\,cm^2\,sr\,\mu m}$ at 1 nm intervals from 380–1,150 nm. SeaWiFS uses spectral responses, not relative spectral responses.

2.2.3 Band-Averaged Spectral Radiance

With finite bandwidths, SeaWiFS can only provide an approximation to the spectral radiance at a single wavelength. For SeaWiFS, the spectral radiance from the measurement is approximated by the band-averaged spectral radiance

$$\overline{L} \;=\; \frac{\displaystyle\int_{\lambda_1}^{\lambda_2} L(\lambda)\, R(\lambda)\, d\lambda}{\displaystyle\int_{\lambda_1}^{\lambda_2} R(\lambda)\, d\lambda}, \tag{9}$$

where the integral in the numerator of (9) represents the radiance the SeaWiFS band measures. This quantity can be described as the moment of the spectral radiance measured, i.e., the sum of the spectral radiances from the source weighted by the distribution of the spectral response.

The integral in the denominator of (9) can have different descriptions, depending on the value of the spectral response that is used, because normalization is accomplished by multiplication by a constant (a constant that makes the maximum value for the RSR equal to unity or a constant that makes the integral of the RSR equal to unity), the normalization has no effect on the results of (9). The same normalization constant is applied to both integrals in the equation, and it can be factored out of both integrals, giving a multiplier of unity to the fraction.

The spectral response, $R(\lambda)$, is defined at each wavelength as the current from the photodiode per unit spectral radiance. For each $L(\lambda)R(\lambda)$ in the upper integral of (9), this product gives the current from the photodiode at that wavelength. The summation of these values of $L(\lambda)R(\lambda)$ (over the wavelength range at which there is a significant instrument response) gives the total current from the photodiode. The postdetector electronics convert the photodiode currents into voltages and then into digital counts.

For the denominator, $L(\lambda)$ is a constant spectral radiance equal to unity. This gives a physical description to the band-averaged spectral radiance in (10),

$$\overline{L} \;=\; \frac{\displaystyle\int_{\lambda_1}^{\lambda_2} L(\lambda)\, R(\lambda)\, d\lambda}{\displaystyle\int_{\lambda_1}^{\lambda_2} L(1)\, R(\lambda)\, d\lambda}, \tag{10}$$

which is functionally equivalent to (9). The output of the instrument divided by the output to a constant source of spectral radiance with a value of unity is given in (10). At the limit of a single wavelength, (10) becomes

$$\overline{L} \;=\; \frac{L(\lambda)}{1}, \tag{11}$$

where the denominator of the ratio represents a spectral radiance of unity.

Other descriptions are also possible; however, the description given here implies there is no spectral dependence in $k_2(g)$. All of the spectral effects are included in the band-averaged spectral radiance. In more physical terms, each SeaWiFS photodiode acts as an integrator of the source radiance. That integration is weighted by the reflecting-transmitting efficiencies of the optical train combined with the conversion efficiency of the diode.

2.2.4 Band-Averaged Center Wavelength

For laboratory measurements, Johnson et al. (1996, 1997, and 1999) used the following definition of center wavelength

$$\lambda_B \;=\; \frac{\displaystyle\int_{\lambda_1}^{\lambda_2} \lambda\, R(\lambda)\, d\lambda}{\displaystyle\int_{\lambda_1}^{\lambda_2} R(\lambda)\, d\lambda}, \tag{12}$$

where λ_B is the band-averaged center wavelength for a source with a constant spectral radiance of unity. The spectral radiance can have any value, so long as it is constant with wavelength, and λ_B will not change. The more general case is given in (13)

$$\lambda_B = \frac{\int_{\lambda_1}^{\lambda_2} \lambda\, L(\lambda)\, R(\lambda)\, d\lambda}{\int_{\lambda_1}^{\lambda_2} L(\lambda)\, R(\lambda)\, d\lambda}. \tag{13}$$

In this case, the spectral shape of the source radiance becomes important to the determination of the center wavelength; (12) and (13) can be described as moments of wavelength. The distribution that provides the moment in (12) is $R(\lambda)$. In (13) the distribution is $L(\lambda)R(\lambda)$. For the SRBC and the transfer-to-orbit experiment, λ_B is of no consequence; only the band-averaged spectral radiance is used. For SeaWiFS measurements in orbit of the upwelling ocean radiance, as modeled by Barnes and Esaias (1997), the band-averaged center wavelengths are given in Table 27 of Barnes (1997). These center wavelengths assume solutions of (13) over the wavelength range from $\lambda_1 = 380\,\text{nm}$ to $\lambda_2 = 1{,}150\,\text{nm}$.

2.2.5 SRBC Basic Equation

If $\overline{L}$ from (9) is substituted for $L(\lambda)$ in (6), the measurement equation becomes

$$\begin{aligned}(DN - DN_0) &= \frac{\overline{L}}{k_2(g)} \\ &= \frac{1}{k_2(g)} \frac{\int_{\lambda_1}^{\lambda_2} L(\lambda)\, R(\lambda)\, d\lambda}{\int_{\lambda_1}^{\lambda_2} R(\lambda)\, d\lambda} \\ &= \frac{1}{k_2(g)} \frac{\int_{\lambda_1}^{\lambda_2} E(\lambda)\, F(\lambda)\, R(\lambda)\, d\lambda}{\int_{\lambda_1}^{\lambda_2} R(\lambda)\, d\lambda},\end{aligned} \tag{14}$$

where, as in (4), $E(\lambda)$ is the solar irradiance at 1 AU—$E(S, \lambda)$, divided by D^2 where D is the Earth–sun distance (in astronomical units) at the time of the measurement. Here, the values at single wavelengths have been replaced by band averages; (14) gives the counts from the instrument for a direct view of the sun in space.

For measurements from the ground, the solar irradiance is attenuated by the transmittance of the atmosphere, $T(\lambda)$; its determination is discussed in Sect. 2.3.3. For ground-based measurements, (14) is modified to become

$$\begin{aligned}(DN - DN_0) &= \frac{\overline{L}}{k_2(g)} \\ &= \frac{1}{k_2(g)} \frac{\int_{\lambda_1}^{\lambda_2} L(\lambda)\, R(\lambda)\, d\lambda}{\int_{\lambda_1}^{\lambda_2} R(\lambda)\, d\lambda} \\ &= \frac{1}{k_2(g)} \frac{\int_{\lambda_1}^{\lambda_2} E(\lambda)\, F(\lambda)\, T(\lambda)\, R(\lambda)\, d\lambda}{\int_{\lambda_1}^{\lambda_2} R(\lambda)\, d\lambda}.\end{aligned} \tag{15}$$

where $T(\lambda)$ is the fractional transmission of the atmosphere at 1 nm intervals (dimensionless). This term is the difference between (14) and (15); The counts from the instrument for a direct view of the sun from the Earth's surface is given in (15). It can be solved for $k_2(g)$, giving

$$\begin{aligned}k_2(g_A) &= \frac{1}{(DN - DN_0)_A} \frac{1}{D_A^2} \\ &\quad \times \frac{\int_{\lambda_1}^{\lambda_2} E(S, \lambda)\; F(\lambda)\, T(\lambda)\, R(\lambda)\, d\lambda}{\int_{\lambda_1}^{\lambda_2} R(\lambda)\, d\lambda}.\end{aligned} \tag{16}$$

In (16), which is the basic equation for the solar radiation-based calibration of SeaWiFS, the calibration coefficient, the net counts from the instrument, and the Earth–sun distance are given the subscript A. Here, the subscript indicates the measurements were made from the ground. In the transfer-to-orbit experiment (Sect. 3), measurements both from the ground and from space are used. There, the ground and space measurements are designated as A and B, respectively.

For the SeaWiFS measurements taken on 1 November 1993, the values of $k_2(g)$ derived from (16) give the solar radiation-based calibration of the instrument. This calibration provides a value for one $k_2(g)$ for each SeaWiFS band. For the SRBC, the reflectance, $F(\lambda)$, is that for the SeaWiFS diffuser cover (Sect. 2.3.4.2), and the atmospheric transmittance is from Sect. 2.3.3. The reflectance spectrum for the diffuser cover is shown in Fig. 2. The SRBC is calculated four times (Sect. 2.6) using, in turn, the solar irradiances from Wehrli (1985), `MODTRAN`, the `6S` model, and Thuillier et al. (1998). Those irradiances are described in Sect. 2.3.2.

2.3 Values in the Integrals

As shown in (16), there are four values within the integrals: the solar irradiance, the BRDF of the diffuser, the transmittance of the atmosphere, and the spectral response of SeaWiFS. The values for the solar irradiances are based

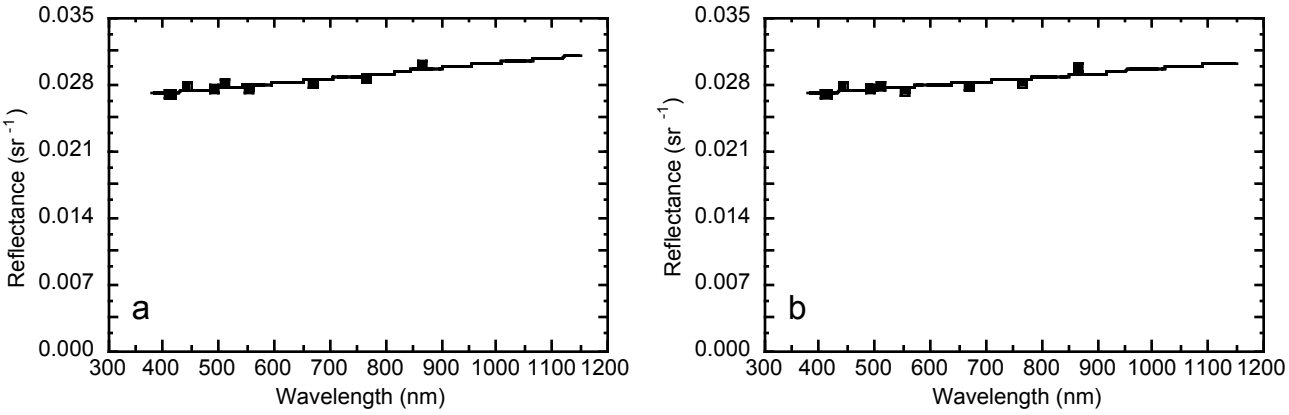

Fig. 2. Reflectances of **a)** the SeaWiFS diffuser, and **b)** the diffuser cover.

on empirical models, that is, on models derived from sets of measurements of the solar flux.

2.3.1 SeaWiFS Spectral Response

The SeaWiFS spectral responses used here are from Barnes (1994). They are derived from the piece parts in the optical trains for the bands (Barnes et al. 1994). For each nanometer in the spectral response tables, the responses have units of picoamperes of current from the photodiode per unit spectral radiance. A unit of spectral radiance is defined as $1\,\mathrm{mW\,cm^{-2}\,sr^{-1}\,\mu m^{-1}}$ (Barnes et al. 1994). The data sets in Barnes (1994) cover the wavelength range from 380–1,150 nm in 1 nm intervals.

A more recent study of the laboratory calibration of SeaWiFS (Barnes and Eplee 1997) showed the wavelength region from 940–1150 nm has very little effect on the band-averaged spectral radiances calculated for the SeaWiFS bands. That study used a radiance source with a color temperature of about 2,850 K, that is, a source with a maximum spectral radiance in the near-infrared at a wavelength near 900 nm. The sun is a source with a peak spectral irradiance near 490 nm and with decreasing spectral irradiance with wavelength over the range from 490–1,150 nm. As a result, it is assumed that, for the calculations presented here, the wavelength region from 940–1,150 nm has very little effect on the band-averaged spectral radiances from the instrument. The spectral responses for the eight SeaWiFS bands are shown in Fig. 3.

2.3.2 Solar Irradiances

Because the integral in the numerator of (16) contains a term for the solar irradiance, there can be a set of calibration coefficients for each solar spectrum used. Here, four solar spectra are used; the calculations can be adapted to use additional spectra.

2.3.2.1 Wehrli

The values in Wehrli (1985) have been compiled from other sources. The principal source of solar irradiances in the regions of the SeaWiFS bands was Neckel and Labs (1984) covering the wavelength range from 380–869 nm. For the remaining SeaWiFS wavelength range, from 870–1,150 nm, Wehrli (1985) used the solar irradiances of Smith and Gottlieb (1974). The spectral resolution of the data in Wehrli (1985) is relatively low: 1 nm from 380–630 nm; 2 nm from 630–1,000 nm; and 5 nm from 1,000–1,150 nm. For the calculations here, the irradiances in the Wehrli model (Fig. 1a) are placed at 1 nm intervals using linear interpolation.

2.3.2.2 `MODTRAN`

The `MODTRAN` model (Berk et al. 1989) gives values at a spectral resolution greater than 1 nm. To obtain values at 1 nm intervals, the `MODTRAN` solar irradiances were averaged using a triangular function with a full width at half maximum of 1 nm. As shown in Fig. 1b, these irradiances show greater structure than those derived from the model of Wehrli (1985), particularly in the two Fraunhofer (solar absorption) lines near 860 nm.

2.3.2.3 `6S`

For the `6S` model (Vermote et al. 1997), the solar irradiances are given at 5 nm intervals. For the calculations here, the irradiances are placed at 1 nm intervals using linear interpolation. The 5 nm resolution of this model gives a plot (Fig. 1c) with a significantly reduced structure than those in Figs. 1a and 1b. In the calculations below, the results using the `6S` solar irradiances are nearly identical with those using the irradiances from the model of Wehrli (1985). This is an indication that, over the wavelength range from 380–1,150 nm, the `6S` irradiances were derived from the same sources used by Wehrli (1985).

2.3.2.4 Thuillier

Figure 1d is derived from the measured values of Thuillier et al. (1998). Those measurements, normalized to 1 AU, are placed at 1 nm intervals using linear interpolation. The Thuillier et al. (1998) measurements extend

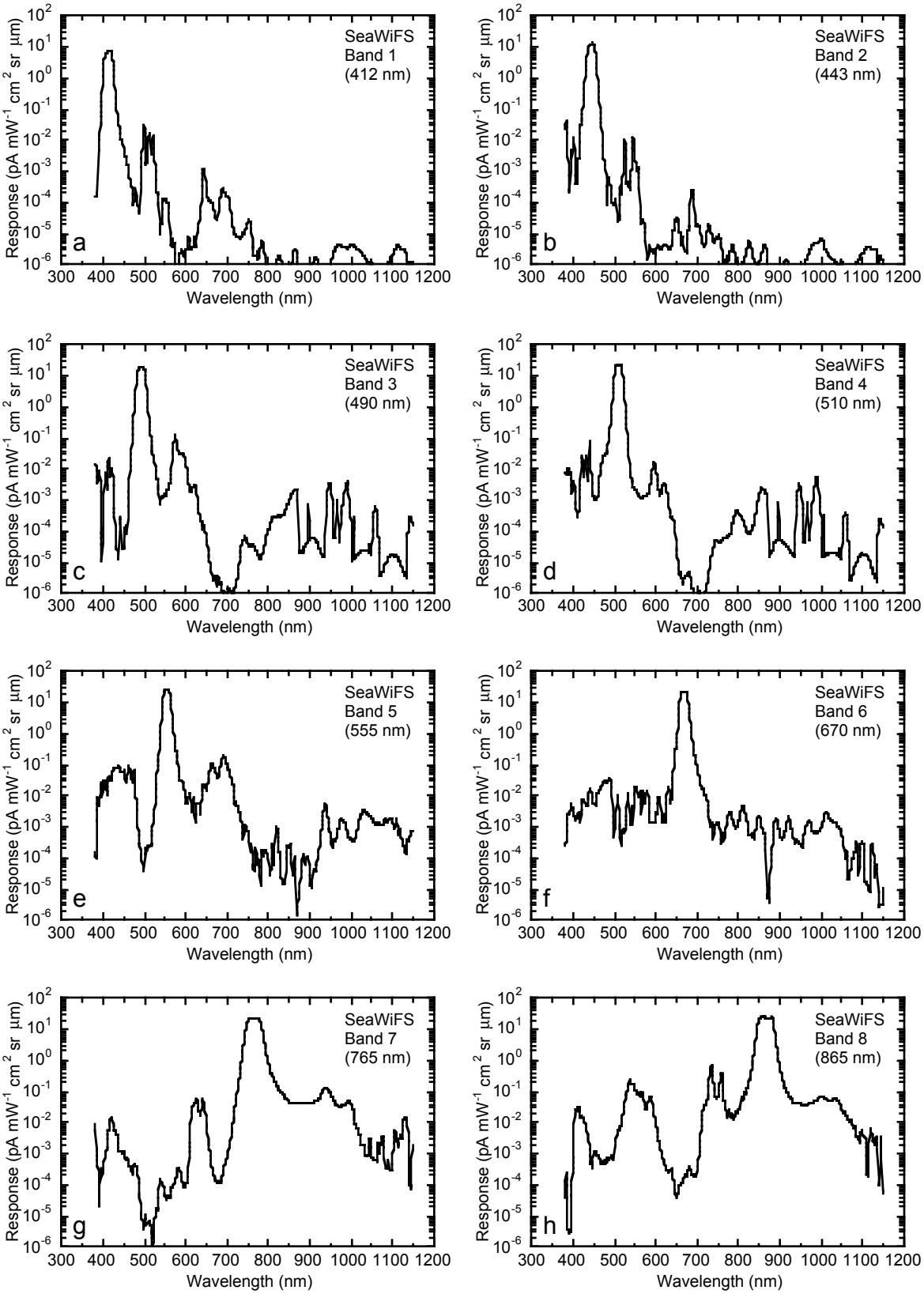

Fig. 3. The spectral responses for the eight SeaWiFS bands. The responses are given from 380–1,150 nm. At each nanometer in this interval, the response has units of picoamperes per unit spectral radiance. As used here, a unit of spectral radiance equals $1\,\mathrm{mW\,cm^{-2}\,sr^{-1}\,\mu m^{-1}}$.

to 880 nm in the near infrared. The Thuillier et al. (1998) data set is extended from 881–1,150 nm using the interpolated values from Wehrli (1985). As stated in Sect. 2.3.1 above, the spectral region from 940–1,150 nm has little effect on the band-averaged spectral radiances from SeaWiFS. The wavelength region around 880 nm, however, falls within the band pass for SeaWiFS band 8 (Fig. 3h). For this reason, the solar radiation-based calibration coefficients using the Thuillier et al. (1998) irradiances are provided for bands 1–7 only.

2.3.3 Atmospheric Transmittance

During the SeaWiFS measurements of the sun on 1 November 1993, the transmittance along the path to the sun was measured with a solar radiometer possessing 10 bands covering the spectral range of about 370–1,040 nm. The transmittance and optical depth results from those measurements are given in Biggar et al. (1995). The sky conditions on 1 November 1993 were not sufficiently favorable to allow a Langley plot determination of the atmospheric transmittance; therefore, instantaneous measurements of the transmittances were made by using previous measurements of the instrument zero-airmass intercept. For calibrations of the solar radiometer done before and after the SRBC, the standard deviation (σ) of the intercepts is about 1% of the intercept value. It is expected that the error in the transmittance measurements on 1 November 1993, when using these intercepts, was approximately 3% or less at the measurement wavelengths.

These measured transmittances, plus measurements of the barometric pressure at the ground, are used to separate the transmittance components due to Rayleigh scattering (scattering by air molecules), and aerosol scattering and absorption (Biggar et al. 1990). The procedure employed here assumes a Junge power law distribution for aerosol particle size. The results on 1 November 1993 gave a Junge parameter of 3.50–3.43 for the measurements. The Rayleigh scattering and aerosol scattering components for atmospheric attenuation are shown in Figs. 4a and 4b. The aerosol component also includes a calculation of the non-zero imaginary part of the refractive index. Figure 4c shows the combined atmospheric transmittance from Rayleigh and aerosol scattering, plus the measurements from the solar radiometer.

After the effects of these components were calculated from the solar radiometer measurements, `MODTRAN` was used to provide the effects of absorption by ozone and other gases. These transmittance spectra are shown in Figs. 4d and 4e. Figure 4d gives the transmittance spectrum for ozone, based on the combined molecular-aerosol transmittance from Fig. 4c, the measurement at 608 nm, and the absorption spectrum for ozone from `MODTRAN`. An ozone amount of 0.246–0.260 atm cm was derived. Figure 4e gives the transmittances for non-ozone gases. For water vapor, the calculation is the same as for ozone, except that the measurement at 940 nm is used. For well mixed atmospheric gases, the transmittance is calculated from the barometric pressure using `MODTRAN`. Only SeaWiFS band 7 exhibits any significant absorption within its pass band, and the oxygen slant path transmittance for band 7 is computed to be 0.927.

These transmittance measurements were made when SeaWiFS was taking data from its illuminated solar diffuser. The results from the transmittance measurements are shown in Fig. 5. The symbols give the transmittances from the solar radiometer measurements, and the curve gives the derived atmospheric transmittance spectrum from 380–1,150 nm in 1 nm intervals. The process of creating Fig. 5 is shown here as a process of sequential calculations. The actual computation, however, is performed as a single mathematical inversion.

2.3.4 BRDF Values

As part of the design of SeaWiFS, a protective cover was placed over the instrument's flight diffuser. The cover was installed to protect the flight diffuser during the initial days of operation in space, when the outgassing of organic and other substances from the instrument and spacecraft could have contaminated the diffuser surface. It was decided to coat the diffuser cover with the same reflective paint as the flight diffuser itself. As a result, SeaWiFS carried two diffusers to orbit. The BRDF values for both diffusers are presented here.

2.3.4.1 Diffuser

The reflectances for the eight SeaWiFS bands are given in Table 1, along with the instrument wavelengths for those measurements. These data are also shown in Fig. 2a. Those wavelengths (for the radiance from an integrating sphere with a color temperature, i.e., a source spectral shape, close to that of a 1,000 W quartz halogen lamp) are taken from Table 25 of Barnes and Eplee (1996).

It is expected that there is little or no structure in the wavelength dependence of the diffuser reflectance. The reflectivity of the YB71 paint on the diffuser is spectrally flat from 400–1,000 nm (Barnes and Eplee 1996). The measurements, as shown in Fig. 2, show a slight, nearly linear spectral dependence in the reflectance of the diffuser; thus, the authors chose to represent the wavelength dependence of the reflectance with the equation

$$y = a_0 + a_1\lambda, \tag{17}$$

where $a_0 = 0.0249988$, $a_1 = 5.19594 \times 10^{-6}$, and λ is the wavelength in nanometers. The fitted values for the reflectances at the SeaWiFS center wavelengths are also given in Table 1, along with the ratio of the fitted values to the measured reflectances. At 1σ, the standard deviation of the ratio is 1.7%.

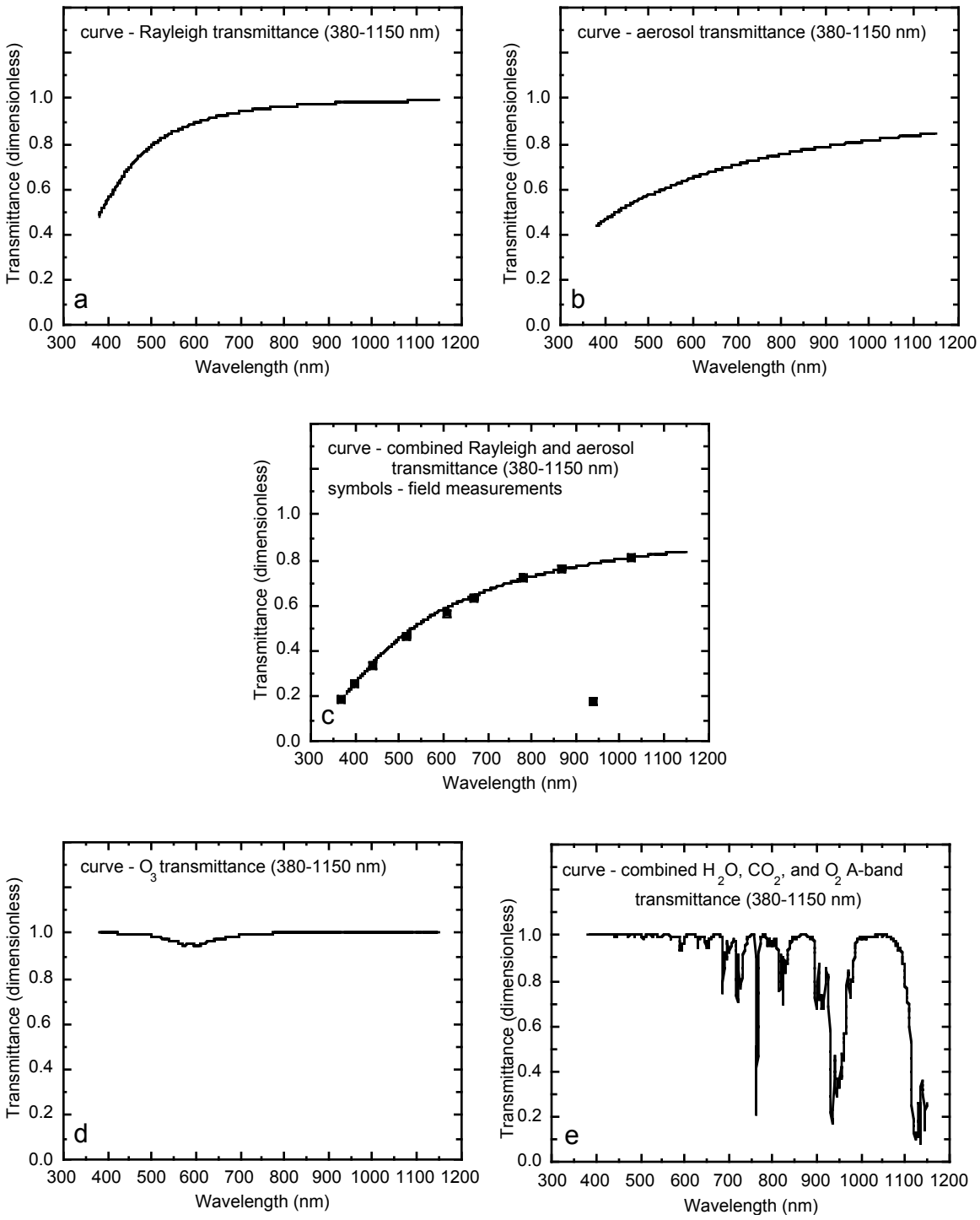

Fig. 4. Atmospheric transmittance components derived from the solar radiometer measurements on 1 November 1993: **a)** transmittance from Rayleigh (molecular) scattering; **b)** transmittance from scattering by aerosols; **c)** combined transmittances from Rayleigh and aerosol and Rayleigh scattering (the symbols give the individual measurements from the solar radiometer); **d)** transmittance from absorption by atmospheric ozone; and **e)** combined transmittances from absorption by water vapor, carbon dioxide, and oxygen at 762 nm (O_2 A-band).

Table 1. The reflectances of the diffuser at the SeaWiFS center wavelengths. The measured reflectances come from Barnes and Eplee (1996). The fitted reflectances are derived using (15).

Band No.	*Center Wavelength* [nm]	*Measured BRDF* [sr^{-1}]	*Fitted BRDF* [sr^{-1}]	*Ratio to Measured*
1	414.5	0.0268	0.0272	1.015
2	444.6	0.0279	0.0273	0.978
3	491.6	0.0275	0.0276	1.004
4	510.5	0.0281	0.0277	0.986
5	555.2	0.0276	0.0279	1.011
6	668.7	0.0280	0.0285	1.018
7	765.7	0.0285	0.0290	1.018
8	866.3	0.0301	0.0295	0.980
			Mean	1.000
			Standard Deviation	0.017

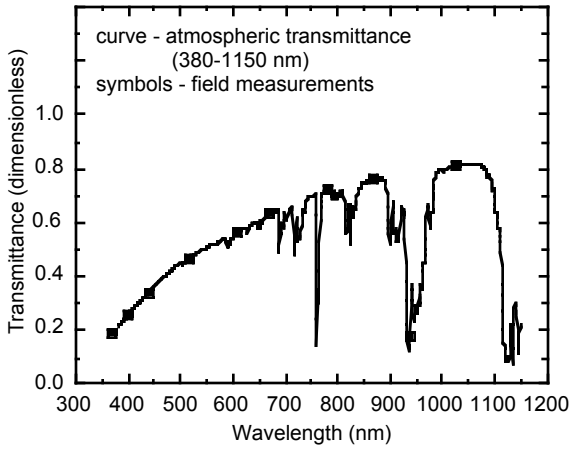

Fig. 5. Atmospheric transmittances during the ground measurements. The symbols give the measurements from the sun photometer. The curve gives the derived atmospheric transmittance spectrum.

2.3.4.2 Diffuser Cover

There were no laboratory measurements of the reflectance of the diffuser cover; however, during the ground measurements (Biggar et al. 1995), the counts from the instrument were taken using the diffuser cover. Immediately afterwards, the diffuser cover was deployed, that is, rotated out of the optical path. Then, counts from the instrument were taken using the diffuser. The diffuser reflectances and the ratios of the diffuser cover counts to the diffuser counts were used to calculate the diffuser cover reflectances. The diffuser cover reflectances are given in Table 2 and plotted in Fig. 2b. The wavelength dependence of the diffuser cover reflectances is also fitted to a linear equation; for the diffuser cover the constants are $a_0 = 0.0254243$ and $a_1 = 4.15626\times10^{-6}$. The fitted values for the reflectances at the SeaWiFS center wavelengths are given in Table 3, along with the ratio of the fitted values to the measured reflectances; at 1σ, the standard deviation of the ratio is 1.7%. The values for the diffuser cover are very close to those of the diffuser itself.

2.3.4.3 Bidirectional Reflectance

The measured values for the reflectances of the SeaWiFS diffuser and diffuser cover in Tables 1 and 2 are given for incident irradiances normal to the plane of the entrance aperture of the diffuser housing. During the laboratory characterization of SeaWiFS, two dimensional reflectance tables, relative to the value at normal incidence, were determined by rotating the instrument while it viewed a halogen lamp via the diffuser (Barnes and Eplee 1996). For incidence angles away from normal, there must be a correction for this angular effect; it can be as large as 5% for a 6° difference from normal (Barnes et al. 1999). For the measurements in the courtyard, a special fixture was used to align the instrument so the solar irradiance was normal to the housing's aperture. This alignment was good at the one-fourth of a degree level (Biggar et al. 1999).

Since the launch of SeaWiFS in August 1997, the diffuser cover has remained in place in the diffuser housing. There has been no need to remove it to expose the flight diffuser. As of this writing, the cover functions as the operational diffuser for the instrument. For the initial on orbit measurement portion of the transfer-to-orbit experiment, solar measurements were made with the diffuser cover. As a result, the authors have decided to use the values from the diffuser cover for the ground portion of the transfer-to-orbit experiment and for the SRBC.

2.4 Ground Measurement Results

The measurements using the diffuser cover are presented in Table 4. These measurements are taken from the 1400 PST measurement sequence on 1 November 1993. The data in the table include the zero offsets for each band (for both the shaded and unshaded measurements); the actual measurements; and two computed values—the ratio of the diffuser signal to the global (or total) signal, and the

Table 2. Values in the calculation of the diffuser cover reflectances.

Band No.	*Center Wavelength* [nm]	*Diffuser BRDF* [sr^{-1}]	*Diffuser Digital Numbers* [$count^{-1}$]	*Diffuser Cover Digital Numbers* [$count^{-1}$]	*Diffuser Cover BRDF* [sr^{-1}]
1	414.5	0.0268	194	195	0.0269
2	444.6	0.0279	236	236	0.0279
3	491.6	0.0275	230	229	0.0274
4	510.5	0.0281	277	275	0.0279
5	555.2	0.0276	361	358	0.0274
6	668.7	0.0280	448	443	0.0277
7	765.7	0.0285	453	447	0.0281
8	866.3	0.0301	533	526	0.0297

Table 3. The reflectances of the diffuser cover at the SeaWiFS center wavelengths. The reflectances come from Table 2. The fitted reflectances are derived using (15).

Band No.	*Center Wavelength* [nm]	*Measured BRDF* [sr^{-1}]	*Fitted BRDF* [sr^{-1}]	*Ratio to Measured*
1	414.5	0.0269	0.0271	1.007
2	444.6	0.0279	0.0273	0.978
3	491.6	0.0274	0.0275	1.004
4	510.5	0.0279	0.0275	0.986
5	555.2	0.0274	0.0277	1.011
6	668.7	0.0277	0.0282	1.018
7	765.7	0.0281	0.0286	1.018
8	866.3	0.0297	0.0290	0.976
			Mean	1.000
			Standard Deviation	0.017

Table 4. SeaWiFS measurements on 1 November 1993 at 1400 PST. Pixel 312 (the center pixel) and pixel 0 (zero offset) were used for determining the total and shaded only signals.

Band No.	*Shaded*		*Unshaded*		*Diffuse:Global*	*Difference of Unshaded From Shaded*
	(Zero Offset)	*(Pixel 312)*	*(Zero Offset)*	*(Pixel 312)*		
1	20	60	20	254	0.17094	194
2	17	58	17	294	0.14801	236
3	20	52	20	282	0.12261	229
4	20	55	20	332	0.11218	277
5	22	60	22	421	0.09520	361
6	24	60	24	508	0.07438	448
7	24	55	24	508	0.06405	453
8	21	58	21	591	0.06491	533

difference between unshaded and shaded measurements. The values in the unshaded versus shaded column give the direct solar beam signals without the diffuse sky contribution. The technique for the measurement of the direct solar beam, including a photograph of the test set up, is given in Biggar et al. (1993a and 1993b). The values in column 7 of Table 4 are the counts, DN, used in the calculations here.

A forward-scatter correction can be made to account for the small amount of forward-scattered diffuse light blocked by the disk. The forward-scatter correction is wavelength dependent, but in all cases it is very small, i.e., less than one count for the atmospheric conditions and the occulting disk size. This correction is not applied to the counts in Table 4, because the correction is less than the resolution of these values.

2.5 Laboratory Results

The primary prelaunch calibration of SeaWiFS was laboratory based. The laboratory calibration coefficients were used by the instrument at the start of its mission on orbit. Those results are an important check on the calibration coefficients from the SRBC.

2.5.1 1997 Calibration

For SeaWiFS, there are four calibration coefficients per band. Table 5 gives those coefficients, derived from the 1997 prelaunch calibration of SeaWiFS. These values are based on Table 19 of Johnson et al. (1999), which gives the calibration coefficients for each channel in each band. There are four channels per band, and, for the measurements presented here, the output from each band is the sum of the output of the individual channels. As a result, the effective calibration coefficient for each band and each gain is given by the equation

$$\frac{1}{k_2(g)} = \frac{1}{4}\left[\frac{1}{k_2(g_1)} + \frac{1}{k_2(g_2)} + \frac{1}{k_2(g_3)} + \frac{1}{k_2(g_4)}\right], \quad (18)$$

where $k_2(g_1)$, $k_2(g_2)$, $k_2(g_3)$, and $k_2(g_4)$ are the calibration constants for gain g, and channels 1–4, respectively; $k_2(g)$ is the effective calibration coefficient for the combined channels.

Table 5. SeaWiFS calibration coefficients derived from Johnson et al. (1999). The coefficients are given for each band and for each of the four instrument gains. The calibration coefficients have units of $\mathrm{mW\,cm^{-2}\,sr^{-1}\,\mu m^{-1}\,count^{-1}}$.

Band No.	$k_2(1)$	$k_2(2)$	$k_2(3)$	$k_2(4)$
1	0.013844	0.007157	0.010623	0.008420
2	0.013426	0.006911	0.010296	0.008133
3	0.010699	0.005478	0.011891	0.006462
4	0.009214	0.004715	0.011600	0.005556
5	0.007614	0.003887	0.011687	0.004829
6	0.004360	0.002212	0.011609	0.006505
7	0.003110	0.001578	0.009638	0.005330
8	0.002224	0.001126	0.008180	0.004387

Table 6. SeaWiFS calibration coefficients derived from Barnes and Eplee (1997 and 1999). The coefficients are given for each band and for each of the four instrument gains. The calibration coefficients have units of $\mathrm{mW\,cm^{-2}\,sr^{-1}\,\mu m^{-1}\,count^{-1}}$.

Band No.	$k_2(1)$	$k_2(2)$	$k_2(3)$	$k_2(4)$
1	0.014201	0.007348	0.010897	0.008647
2	0.013541	0.006978	0.010391	0.008213
3	0.010665	0.005456	0.011842	0.006436
4	0.009189	0.004698	0.011564	0.005537
5	0.007483	0.003812	0.011488	0.004738
6	0.004226	0.002144	0.011247	0.006303
7	0.003012	0.001527	0.009332	0.005168
8	0.002137	0.001082	0.007872	0.004221

2.5.2 1993 Calibration

The calibration values from Table 25 in Barnes and Eplee (1997) are used to create the calibration coefficients here. The procedure used, based on (18), is the same as that used with the 1997 calibration data from Johnson et al. (1999). The values in Table 6 are given in the same format as those in Table 5.

2.6 Field and Laboratory Comparisons

The solutions to (16) include the calculation of the band-averaged spectral radiance. The terms in this calculation come from the values described in Sects. 2.3.2, 2.3.3, and 2.3.4. The ratio of integrals is cumbersome to use in the headers of the tables that follow. As a result, the term $\overline{L}_G(\lambda)$ is defined as

$$\overline{L}_G(\lambda) = \frac{\int_{\lambda_1}^{\lambda_2} E(S,\lambda)\; T(\lambda)\, R(\lambda)\, d\lambda}{\int_{\lambda_1}^{\lambda_2} R(\lambda)\, d\lambda}, \quad (19)$$

where $\overline{L}_G(\lambda)$ is the band-averaged spectral radiance for the ground measurement. There are four solutions given for $\overline{L}_G(\lambda)$, below, one for each of the solar irradiance models.

2.6.1 Wehrli Irradiances

Table 7 gives the solutions to (16) using the solar irradiances, $E(S,\lambda)$ from Wehrli (1985) as shown in Fig. 1a. The solutions use the reflectances, $F(\lambda)$, for the diffuser cover from Fig. 2b and the atmospheric transmittances, $T(\lambda)$, from Fig. 5. The solutions also use the spectral responses, $R(\lambda)$, of the SeaWiFS bands. For the measurements on 1 November 1993, the Earth–sun distance (D_A) was 0.9923 AU, and the net counts from the instrument are given in Table 2.

Table 7 also gives the SeaWiFS gains used for the measurements and the calculated calibration coefficients from the SRBC. In Table 7, there is one calibration coefficient per band. These calibration coefficients from the SRBC are also listed in Table 8, which are in the same format as those from the laboratory calibrations in Tables 5 and 6.

In Table 9, the SRBC calibration coefficients, based on the solar irradiances from Wehrli (1985), are compared with the corresponding calibration coefficients from the laboratory calibrations. In general, these SRBC calibration coefficients are 1–5% lower than the laboratory values; and the comparison with the 1993 laboratory calibration coefficients is better than that with the laboratory calibration coefficients from 1997.

The comparison results are shown in Fig. 6. The figure has horizontal reference lines at 0.97, 1, and 1.03. These are visual references for the comparison results. In Fig. 6a, the Wehrli-based calibration coefficients are plotted as their ratios to the calibration coefficients from the 1997 laboratory calibration of the instrument (Johnson et al. 1999). In Fig. 6b, the Wehrli coefficients (squares) are plotted as their ratios to the coefficients from the 1993

Table 7. SeaWiFS calibration coefficients derived from the field measurements on 1 November 1993. One calibration coefficient, $k_2(g)$, is given for each band. The coefficients have units of $\mathrm{mW\,cm^{-2}\,sr^{-1}\,\mu m^{-1}\,count^{-1}}$. The calculation uses the solar irradiance model of Wehrli (1985). The term $\overline{L}_G(\lambda)$ represents the band-averaged spectral radiance, and it is defined in (19).

Band No.	$\overline{L}_G(\lambda)$ *(Wehrli)*	D_A	$\overline{L}_G(\lambda)/D_A^2$	$(DN - DN_0)_A$	g	$k_2(g)$ *(Wehrli)*
1	1.34517	0.9923	1.36613	195	2	0.007006
2	1.82766	0.9923	1.85614	236	4	0.007865
3	2.31511	0.9923	2.35118	229	1	0.010267
4	2.38617	0.9923	2.42334	275	1	0.008812
5	2.62476	0.9923	2.66566	358	1	0.007446
6	2.72128	0.9923	2.76367	443	4	0.006239
7	2.23197	0.9923	2.26675	447	4	0.005071
8	2.14928	0.9923	2.18277	526	4	0.004150

Table 8. SeaWiFS calibration coefficients derived from the field measurements on 1 November 1993. The calibration coefficients have units of $\mathrm{mW\,cm^{-2}\,sr^{-1}\,\mu m^{-1}\,count^{-1}}$; the coefficients come from Table 7. The format of this table is the same as for Tables 5 and 6.

Band No.	$k_2(1)$	$k_2(2)$	$k_2(3)$	$k_2(4)$
1		0.007006		
2				0.007865
3	0.010267			
4	0.008812			
5	0.007446			
6				0.006239
7				0.005071
8				0.004150

Table 9. Comparison of the SRBC coefficients with those from the 1997 and 1993 laboratory calibrations of SeaWiFS. The calibration coefficients have units of $\mathrm{mW\,cm^{-2}\,sr^{-1}\,\mu m^{-1}\,count^{-1}}$. The coefficients under k_2 SRBC (Wehrli) come from Table 7. The coefficients under k_2 Lab (1997) come from Table 5, and those under k_2 Lab (1993) come from Table 6.

Band No.	k_2 *SRBC (Wehrli)*	k_2 *Lab. (1997)*	*Ratio to* k_2 *Lab. (1997)*	k_2 *Lab. (1993)*	*Ratio to* k_2 *Lab. (1993)*
1	0.007006	0.007157	0.979	0.007348	0.954
2	0.007865	0.008133	0.967	0.008213	0.958
3	0.010267	0.010699	0.960	0.010665	0.963
4	0.008812	0.009214	0.956	0.009189	0.959
5	0.007446	0.007614	0.978	0.007483	0.995
6	0.006239	0.006505	0.959	0.006303	0.990
7	0.005071	0.005330	0.951	0.005168	0.982
8	0.004150	0.004387	0.946	0.004221	0.984
		Mean	0.962		0.972
		Standard deviation	0.012		0.016

laboratory calibration found in Barnes and Eplee (1997). In Fig. 6a, the Wehrli-based calibration coefficients average about 4% lower than those from the 1997 laboratory calibration. For the comparison with the 1993 laboratory calibration in Fig. 6b, the Wehrli values average about 3% lower.

A comparison of the coefficients from the 1993 and 1997 laboratory calibration of SeaWiFS is shown in Fig. 7. The results of the 1997 calibration are shown as ratios to those from 1993. There is an upward slope in Fig. 7 with increasing band number from bands 1–8. Because the laboratory calibrations are part of the denominators of the ratios in Figs. 6a and 6b, there is a slight downward slope with band number for the Wehrli-based comparison in Fig. 6a, and a slight upward slope with band number for the comparison in Fig. 6b.

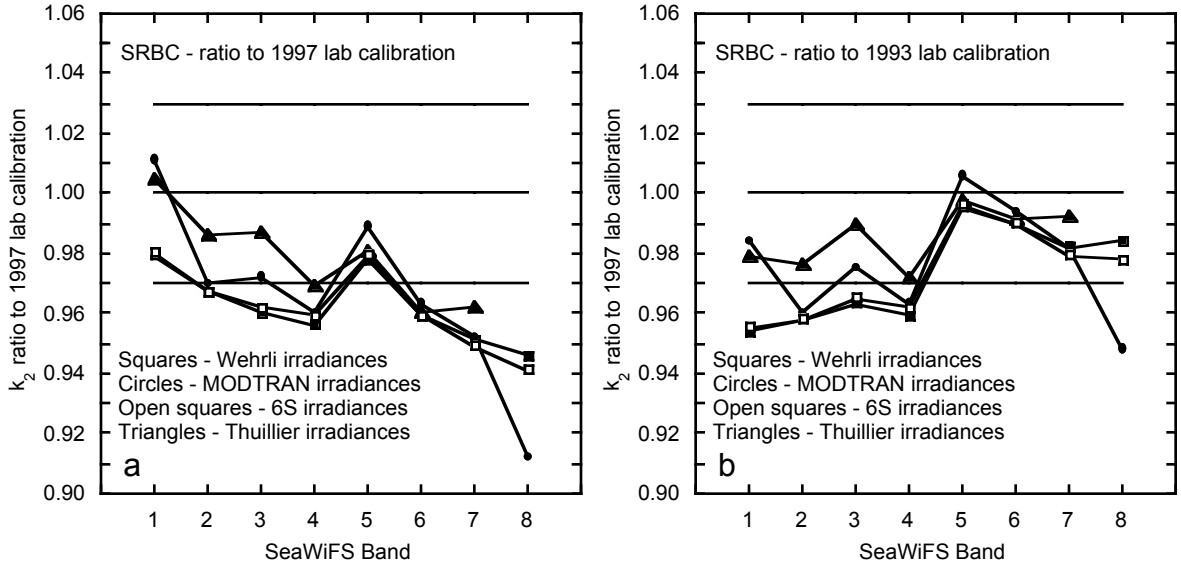

Fig. 6. Comparison of the coefficients (k_2) from the SRBC with those from the laboratory calibrations. The squares give the comparison using the Wehrli irradiances; the circles give the comparison using the `MODTRAN` irradiances; and the triangles give the Thuillier values. **a)** Comparison of the SRBC coefficients with those from the 1997 laboratory calibration. **b)** Comparison of the SRBC coefficients with those from the 1993 laboratory calibration.

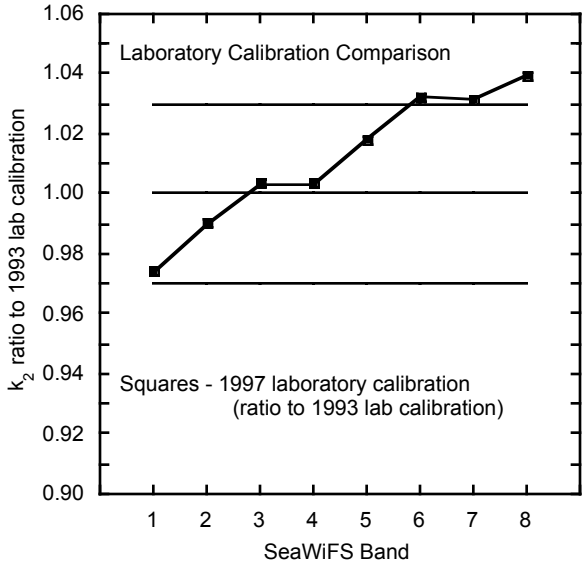

Fig. 7. A comparison of the 1997 laboratory-based calibration coefficients, $k_2(g)$, for SeaWiFS with those from the 1993 laboratory calibration.

2.6.2 MODTRAN Irradiances

Table 10 gives the solutions to (16) using the solar irradiances, $E(S,\lambda)$, from MODTRAN as shown in Fig. 1b; in other respects, the solutions to the equation are the same as those in Sect. 2.6.1.

In Table 11, the SRBC calibration coefficients, based on the solar irradiances from MODTRAN, are compared with the corresponding calibration coefficients from the laboratory calibrations. On the average, the agreement between the MODTRAN SRBC calibration coefficients with the laboratory values in Table 11 is about the same as that for the Wehrli comparisons in Table 9. The MODTRAN-based calibration coefficients, however, show slopes with band number (and, thus, with wavelength) with respect to the laboratory-based coefficients which are not seen in the Wehrli-laboratory comparisons.

Without the comparison values for band 8, the skew in the comparison of the MODTRAN values (circles) with the 1997 laboratory calibration in Fig. 6a is much less pronounced. The difference in the values for band 8 in Figs. 6a and 6b compared with the Wehrli values, arises in large part from the different magnitudes of the Fraunhofer lines at 854 nm and 866 nm in the solar irradiance spectra in Figs. 1a and 1b. These Fraunhofer lines occur in the pass band for SeaWiFS band 8 (Fig. 3h). In the MODTRAN solar irradiances, these Fraunhofer absorptions decrease the solar irradiance by about 15–20%. In the Wehrli (1985) spectrum, these lines are less pronounced.

2.6.3 6S Irradiances

Table 12 gives the solutions to (16) using the solar irradiances, $E(S,\lambda)$, from the 6S model (Vermote et al. 1997). The values of $\overline{L}_G(\lambda)$ in Table 12 are very close to those in Table 7 (0.3% or better for bands 1–7 and 0.5% for band 8). From this evidence, the authors concluded that the Wehrli and 6S irradiance spectra are based on those of Neckel and Labs (1984). For wavelengths from 870–1,150 nm, it appears the 6S irradiances are also based on those of Neckel and Labs (1984), while the Wehrli solar irradiances are taken from those of Smith and Gottlieb (1974).

The analysis of Barnes and Eplee (1997) found the wavelength region from 940–1,150 nm to have very little effect on band-averaged spectral radiances calculated for the SeaWiFS bands. In addition, the 5 nm resolution of the 6S solar irradiances appears to cause the majority of the differences between the SRBC values based on 6S and Wehrli. For SeaWiFS measurements, therefore, the 6S and Wehrli solar irradiances are considered functionally the same. The SRBC results using the 6S solar irradiances are presented in Tables 12 and 13, and the comparisons with the laboratory measurements are shown in Fig. 6; however, these results are not independent of those using the irradiances of Wehrli.

2.6.4 Thuillier Irradiances

As discussed in Sect. 2.3.2.4, the Thuillier et al. (1998) solar irradiances extend to 870 nm only. To provide a spectrum covering the wavelength range for the SeaWiFS spectral responses, the solar irradiances from Wehrli (1985) are used from 871–1,150 nm. Since the Thuillier et al. (1998) irradiances end in the middle of the pass band of SeaWiFS band 8 (Fig. 3h), the SRBC coefficient for band 8 is not included here. Table 14 gives the solutions to (16) using the solar irradiances, $E(S,\lambda)$, from Thuillier et al. (1998) as shown in Fig. 1d. On the average, the agreement between the Thuillier-based SRBC calibration coefficients with the laboratory values in Table 15 is about 1–1.5% better than that for the Wehrli-based coefficients in Table 9. This agreement is also shown in Figs. 6a and 6b. As with the SBRC coefficients using the other solar irradiances, the agreement of the Thuillier et al. (1998) coefficients is better with the 1993 laboratory calibration than with the calibration in 1997. The comparisons using the Thuillier-based solar irradiances, however, include only seven of the eight SeaWiFS bands.

2.7 Band-Averaged Solar Irradiances

The integrals in (16) and those used in its development are solved as summations. As such, the equations can be separated and *band averaged* as individual parts. In the calculations, the summation is done using a series of histograms. Because the values of the histograms at the ends of the summations are very close to zero, this technique is equivalent to a trapezoidal integration. The band-averaged solar irradiance (at 1 AU) is calculated from solar models using

$$E_B = \frac{\sum_{\lambda=\lambda_1}^{\lambda_2} E(\lambda)\, R(\lambda)\, \Delta\lambda}{\sum_{\lambda=\lambda_1}^{\lambda_2} R(\lambda)\, \Delta\lambda}, \qquad (20)$$

where the increment, $\Delta\lambda$, is 1 nm. This formulation is equivalent to that for band-averaged spectral radiance in (9). It is also possible to calculate a band-averaged BRDF, F_B, and a band-averaged atmospheric transmittance, T_B. Because (16) includes the product of three band-averaged factors (E_B, F_B, and T_B), a given fractional change in any of these factors will cause an identical fractional change in $k_2(g)$.

2.7.1 Irradiance Comparisons

The SeaWiFS atmospheric correction algorithm uses band-averaged solar irradiances. These values are based on the solar model of Neckel and Labs (1984), and are given in Table 16 under the column header "SeaWiFS." The SeaWiFS values were calculated elsewhere. Table 16

Table 10. SeaWiFS calibration coefficients derived from the field measurements on 1 November 1993. One calibration coefficient, $k_2(g)$, is given for each band. The coefficients have units of $\mathrm{mW\,cm^{-2}\,sr^{-1}\,\mu m^{-1}\,count^{-1}}$. The calculation uses the solar irradiance model from MODTRAN. The term $\overline{L}_G(\lambda)$ represents the band-averaged spectral radiance, and is defined in (19).

Band No.	$\overline{L}_G(\lambda)$ (MODTRAN)	D_A	$\overline{L}_G(\lambda)/D_A^2$	$(DN - DN_0)_A$	g	$k_2(g)$ (MODTRAN)
1	1.38884	0.9923	1.41048	195	2	0.007233
2	1.83260	0.9923	1.86116	236	4	0.007886
3	2.34522	0.9923	2.38175	229	1	0.010401
4	2.39642	0.9923	2.43376	275	1	0.008850
5	2.65350	0.9923	2.69484	358	1	0.007527
6	2.73318	0.9923	2.77576	443	4	0.006266
7	2.23393	0.9923	2.26874	447	4	0.005075
8	2.07201	0.9923	2.10429	526	4	0.004001

Table 11. Comparison of the SRBC coefficients with those from the 1997 and 1993 laboratory calibrations of SeaWiFS. The calibration coefficients have units of $\mathrm{mW\,cm^{-2}\,sr^{-1}\,\mu m^{-1}\,count^{-1}}$. The coefficients under "k_2 SRBC (MODTRAN)" come from Table 10. The coefficients under "k_2 Lab (1997)" come from Table 5, and those under "k_2 Lab (1993)" come from Table 6.

Band No.	*k_2 SRBC* (MODTRAN)	*k_2 Lab. (1997)*	*Ratio to k_2 Lab. (1997)*	*k_2 Lab. (1993)*	*Ratio to k_2 Lab. (1993)*
1	0.007233	0.007157	1.011	0.007348	0.984
2	0.007886	0.008133	0.970	0.008213	0.960
3	0.010401	0.010699	0.972	0.010665	0.975
4	0.008850	0.009214	0.960	0.009189	0.963
5	0.007527	0.007614	0.989	0.007483	1.006
6	0.006266	0.006505	0.963	0.006303	0.994
7	0.005075	0.005330	0.952	0.005168	0.982
8	0.004001	0.004387	0.912	0.004221	0.948
		Mean	0.966		0.977
		Standard Deviation	0.029		0.019

Table 12. SeaWiFS calibration coefficients derived from the field measurements on 1 November 1993. One calibration coefficient, $k_2(g)$, is given for each band. The coefficients have units of $\mathrm{mW\,cm^{-2}\,sr^{-1}\,\mu m^{-1}\,count^{-1}}$. The calculation uses the 6S solar irradiance model. The term $\overline{L}_G(\lambda)$ represents the band-averaged spectral radiance, and is defined in (19).

Band No.	$\overline{L}_G(\lambda)$ (6S)	D_A	$\overline{L}_G(\lambda)/D_A^2$	$(DN - DN_0)_A$	g	$k_2(g)$ (6S)
1	1.34687	0.9923	1.36786	195	2	0.007015
2	1.82821	0.9923	1.85669	236	4	0.007867
3	2.31975	0.9923	2.35589	229	1	0.010288
4	2.39279	0.9923	2.43007	275	1	0.008837
5	2.62847	0.9923	2.66942	358	1	0.007456
6	2.72258	0.9923	2.76499	443	4	0.006242
7	2.22688	0.9923	2.26158	447	4	0.005059
8	2.13785	0.9923	2.17116	526	4	0.004128

Table 13. Comparison of the SRBC coefficients with those from the 1997 and 1993 laboratory calibrations of SeaWiFS. The calibration coefficients have units of $\mathrm{mW\,cm^{-2}\,sr^{-1}\,\mu m^{-1}\,count^{-1}}$. The coefficients under "k_2 SRBC (6S)" come from Table 12. The coefficients under"k_2 Lab (1997)" come from Table 5, and those under "k_2 Lab (1993)" come from Table 6.

Band No.	*k_2 SRBC (6S)*	*k_2 Lab. (1997)*	*Ratio to k_2 Lab. (1997)*	*k_2 Lab. (1993)*	*Ratio to k_2 Lab. (1993)*
1	0.007015	0.007157	0.980	0.007348	0.955
2	0.007867	0.008133	0.967	0.008213	0.958
3	0.010288	0.010699	0.962	0.010665	0.965
4	0.008837	0.009214	0.959	0.009189	0.962
5	0.007456	0.007614	0.979	0.007483	0.996
6	0.006242	0.006505	0.959	0.006303	0.990
7	0.005059	0.005330	0.949	0.005168	0.979
8	0.004128	0.004387	0.941	0.004221	0.978
		Mean	0.962		0.973
		Standard Deviation	0.013		0.014

Table 14. SeaWiFS calibration coefficients derived from the field measurements on 1 November 1993. One calibration coefficient, $k_2(g)$, is given for each band. The coefficients have units of $\mathrm{mW\,cm^{-2}\,sr^{-1}\,\mu m^{-1}\,count^{-1}}$. The calculation uses the solar irradiance measurements from Thuillier (1999). The term $\overline{L}_G(\lambda)$ represents the band-averaged spectral radiance, and is defined in (19). Thuillier's data do not cover the wavelength range for band 8.

Band No.	$\overline{L}_G(\lambda)$ (Thuillier)	D_A	$\overline{L}_G(\lambda)/D_A^2$	$(DN - DN_0)_A$	g	$k_2(g)$ (Thuillier)
1	1.38132	0.9923	1.40284	195	2	0.007194
2	1.86340	0.9923	1.89243	236	4	0.008019
3	2.38140	0.9923	2.41850	229	1	0.010561
4	2.41744	0.9923	2.45511	275	1	0.008928
5	2.63230	0.9923	2.67331	358	1	0.007467
6	2.72356	0.9923	2.76599	443	4	0.006244
7	2.25625	0.9923	2.29140	447	4	0.005126
8						

Table 15. Comparison of the SRBC coefficients with those from the 1997 and 1993 laboratory calibrations of SeaWiFS. The calibration coefficients have units of $\mathrm{mW\,cm^{-2}\,sr^{-1}\,\mu m^{-1}\,count^{-1}}$. The coefficients under k_2 SRBC (Thuillier) come from Table 13. The coefficients under k_2 Lab (1997) come from Table 5, and those under k_2 Lab (1993) come from Table 6. Thuillier's data do not cover the wavelength range for band 8.

Band No.	*k_2 SRBC (Thuillier)*	*k_2 Lab. (1997)*	*Ratio to k_2 Lab. (1997)*	*k_2 Lab. (1993)*	*Ratio to k_2 Lab. (1993)*
1	0.007194	0.007157	1.005	0.007348	0.979
2	0.008019	0.008133	0.986	0.008213	0.976
3	0.010561	0.010699	0.987	0.010665	0.990
4	0.008928	0.009214	0.969	0.009189	0.972
5	0.007467	0.007614	0.981	0.007483	0.998
6	0.006244	0.006505	0.960	0.006303	0.991
7	0.005126	0.005330	0.962	0.005168	0.992
8					
		Mean	0.979		0.985
		Standard Deviation	0.016		0.010

Table 16. Solar irradiances. The SeaWiFS irradiances come from the SeaWiFS atmospheric correction code which was current as of 1 February 1999. The solar irradiances for Wehrli, MODTRAN, 6S, and Thuillier are calculated using (18); the irradiances have units of $\mathrm{mW\,cm^{-2}\,sr^{-1}\,\mu m^{-1}}$. The SeaWiFS irradiances are listed in the atmospheric correction code with a resolution of 0.01 spectral irradiance unit.

Band No.	SeaWiFS	Wehrli	MODTRAN	6S	Thuillier
1	170.79	170.554	176.277	170.736	175.214
2	189.45	189.226	189.702	189.283	192.867
3	193.66	193.424	195.991	193.810	198.999
4	188.35	188.133	188.958	188.652	190.655
5	185.33	185.066	187.088	185.326	185.628
6	153.41	153.204	153.877	153.282	153.341
7	122.24	122.487	122.646	122.221	124.003
8	98.82	99.396	95.872	98.880	

also includes band-averaged solar irradiances calculated using (20) and the model results in Fig. 1. The Wehrli values in Table 16 are very close to the SeaWiFS irradiances, as are the values from 6S.

Table 17 gives the band-averaged solar irradiances for the solar models normalized to the corresponding value in the SeaWiFS atmospheric correction. The set of values in Table 17 agree with the SeaWiFS irradiance, and with each other, at the 3.5% level. The SRBC results in Figs. 6a and 6b, also show an agreement at the 3.5% level.

Table 17. Normalized solar irradiances. The Wehrli, MODTRAN, 6S, and Thuillier solar irradiances in Table 14 are normalized to the corresponding SeaWiFS irradiance.

Band No.	Wehrli	MODTRAN	6S	Thuillier
1	0.999	1.032	1.000	1.026
2	0.999	1.001	0.999	1.018
3	0.999	1.012	1.001	1.028
4	0.999	1.003	1.002	1.012
5	0.999	1.009	1.000	1.002
6	0.999	1.003	0.999	1.000
7	1.002	1.003	1.000	1.014
8	1.006	0.970	1.001	

2.7.2 Fraunhofer Lines

SeaWiFS band 8 contains two solar lines at 854–866 nm within its pass band. These two Fraunhofer lines, plus a less intense one at 850 nm, come from the absorption of upwelling solar flux by calcium within the atmosphere of the sun (Lang 1980). As shown in Fig. 1, the four solar models include these lines, each model with different line widths and intensities. A detailed plot of the spectral response of SeaWiFS band 8 is shown in Fig. 8. It covers the region between the wavelengths at which the response of the band is 1% of its maximum, or greater. These wavelengths, 826 nm and 908 nm, are the extended band edges and they mark the limits of the in-band response for the band (Barnes et al. 1994).

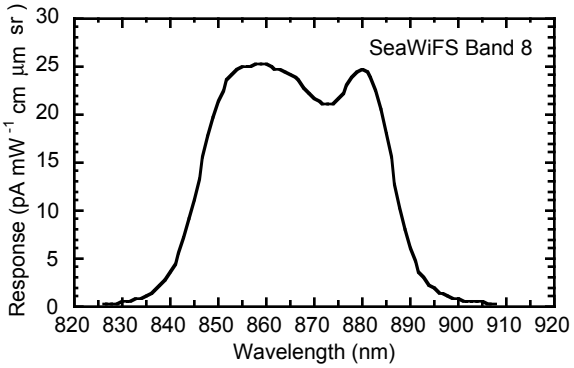

Fig. 8. The spectral response for SeaWiFS band 8. This spectrum covers the wavelength range from 826–908 nm, i.e., the in-band response region.

Figure 9a shows the Wehrli solar irradiances over the same wavelength range as band 8 in Fig. 8. With the values in Figs. 8 and 9a, it is possible to calculate the SeaWiFS band-averaged solar irradiance using (20); this value is listed in Table 18. Figure 9b shows the Wehrli irradiances with the Fraunhofer lines removed. The lines were replaced with linear interpolations across their bases. The band-averaged solar irradiance for this spectrum is also given in Table 18. In a similar manner, the solar irradiances for the MODTRAN, 6S, and Thuillier solar models are presented, with and without their Fraunhofer lines. The solar irradiances in Table 18 are not the same as those for band 8 in Table 16. They are smaller by about 0.8% than the band-averaged irradiances calculated over the wavelength range from 380–1,150 nm. SeaWiFS band 8 has a significant out-of-band response for wavelengths from 700–750 nm (Fig. 3). This response, combined with the solar irradiance, is sufficient to increase the band-averaged solar irradiance by almost 1%. For the Thuillier irradiances in Figs. 9g and 9h, the values from 871–908 nm were taken from Wehrli (1985).

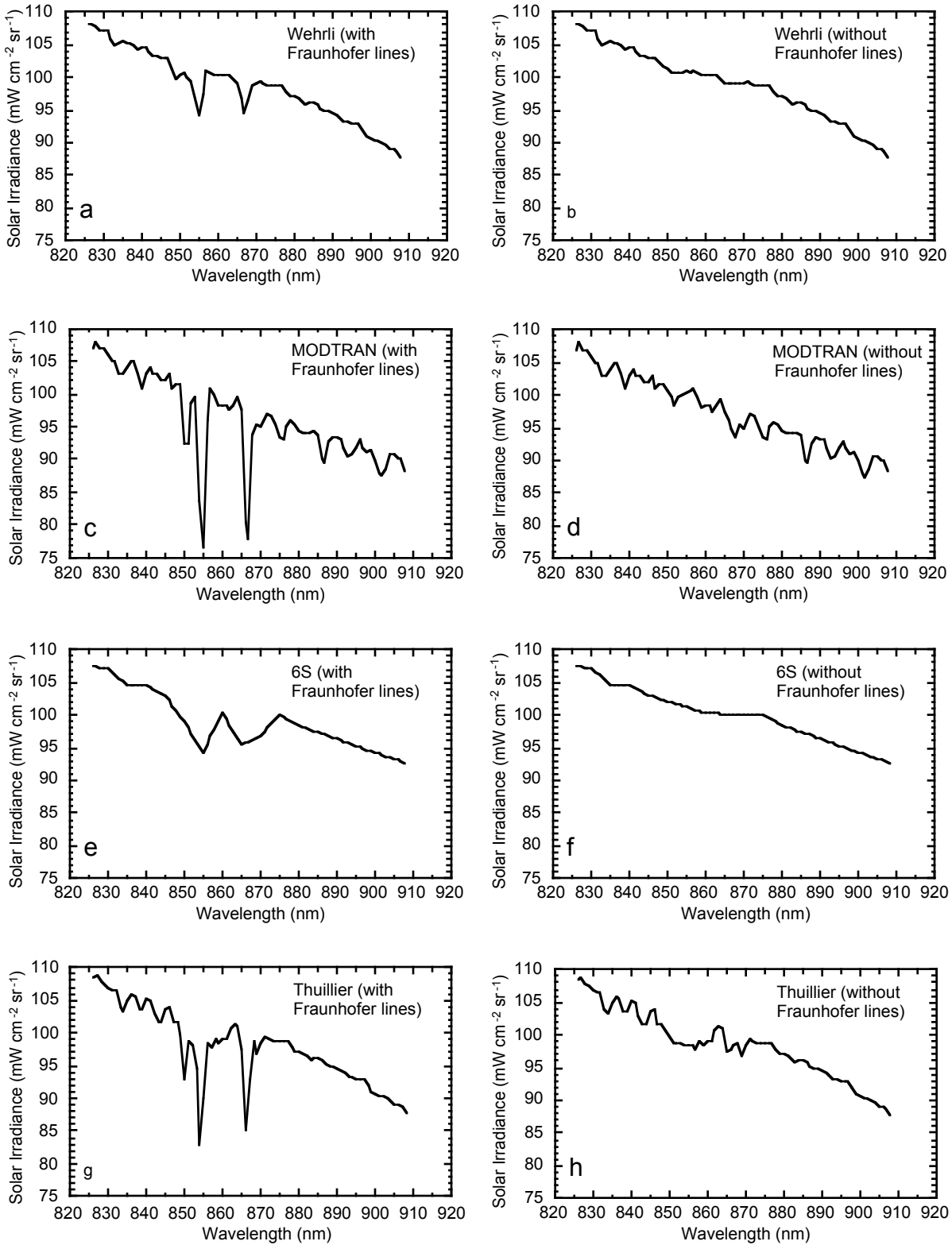

Fig. 9. Irradiances from the Wehrli, MODTRAN, 6S, and Thuillier solar models. The wavelengths for these spectra cover the in-band response range for SeaWiFS band 8 (Fig. 8). The left hand panels for each solar model shows the irradiances with the Fraunhofer lines included. The right hand panels shows the irradiances with the lines removed.

Table 18. Solar irradiance values are given with and without Fraunhofer lines for SeaWiFS band 8. The irradiances are calculated for the band response curve in Fig. 8. The solar irradiance curves for these calculations are shown in Fig. 9; the irradiances have units of $\mathrm{mW\,cm^{-2}\,\mu m^{-1}}$. The ratios are the values of the irradiances for spectra without Fraunhofer lines to the irradiances to the spectra with Fraunhofer lines.

Fraunhofer Lines	Wehrli	MODTRAN	6S	Thuillier
Lines	98.622	94.989	97.328	98.069
No Lines	99.314	97.142	98.595	100.097
Ratio	1.007	1.023	1.013	1.021

Eliminating the Fraunhofer lines changes the band-averaged spectral irradiances, for SeaWiFS band 8, by amounts ranging from 0.7% (using the Wehrli irradiances) to 2.3% (using the MODTRAN irradiances). The Thuillier solar model, using recent measurements from orbit on the Space Shuttle (Thuillier et al. 1998), shows Fraunhofer lines with widths and strengths that are similar to those from the MODTRAN model. The consistency of the Thuillier and MODTRAN data leads to the conclusion that, for the band-averaged spectral irradiance for SeaWiFS band 8, the Wehrli (1985) solar model underestimates the effect of the Fraunhofer lines at 854 nm and 866 nm by about 1.5%. In addition, the 6S model underestimates the same effect by about 1%. It should be noted that the Fraunhofer effects are independent of the absolute value of the radiance continuum to which these features are attached.

2.8 Discussion

The prelaunch calibration coefficients used by SeaWiFS come from the 1997 calibration of the instrument (Johnson et al. 1999). Those coefficients agree with those from the manufacturer in 1993 (Barnes and Eplee 1997) at the 4% level with the greatest difference in band 8. This agreement is within the 5% calibration accuracy requirement in the specifications for the SeaWiFS instrument.

The SRBC of SeaWiFS requires the use of a model solar irradiance spectrum. Using the solar models of Wehrli (1985), MODTRAN (Berk et al. 1989), 6S (Vermote et al. 1997) and Thuillier et al. (1998), the calibration coefficients from the SRBC agree at the 3.6% level with the greatest difference in band 8. This statistic is a measure of the maximum difference between the irradiances for the solar models when they are averaged using the spectral responses of the SeaWiFS bands.

In Fig. 6a, the SRBC calibration coefficients are compared with those from the 1997 laboratory calibration of SeaWiFS. For the SRBC using the Wehrli irradiances, the average difference from the laboratory calibration is 3.8% with a 1.2% standard deviation. When expressed in terms of the ratio of the SRBC calibration coefficients to those from the laboratory in 1997, the average is 0.962±0.012. In all cases, the Wehrli-based calibration coefficients are lower than those from the laboratory with a maximum difference of 5.4% for band 8. For the other solar models, the SRBC results are also consistently low. For the comparison of the SRBC and laboratory calibrations of SeaWiFS, the Wehrli-based results are considered to be representative of those from the set of solar models.

For the MODTRAN irradiances, the ratios of the calibration coefficients to those from the 1997 laboratory calibration average 0.966±0.029; for the 6S irradiances, the average is 0.963±0.013; and for the Thuillier irradiances, the average is 0.979±0.016. The 6S irradiances are, however, for practical purposes, the same as those from the Wehrli solar model. In addition, the Thuillier calibration coefficients do not include band 8.

There are several uncertainties in the SRBC that are separate from the uncertainties in the solar models. The first is the uncertainty in the atmospheric transmission, which the authors estimate to be about 3% (Biggar et al. 1993a, 1993b, and 1999). The second is the uncertainty in the knowledge of the reflectance of the diffuser cover. The authors estimate this to be about 4%. For the diffuser, there is a small additional uncertainty of 0.4% for the alignment of the diffuser with the sun (Biggar et al. 1999). The fourth uncertainty comes from the possible change in the instrument between the time of the solar calibration in 1993 and the laboratory calibration in 1997. This uncertainty is estimated to be about 2 or 3% (Sect. 3.4). For these uncertainties, the square root of the sum of the squares is about 5 or 6%.

3. TRANSFER TO ORBIT

This experiment makes use of the same ground-based measurements as the SRBC. These values are used in a two part process to determine changes in the instrument. As a result, the absolute values for the calibration coefficients and the BRDF of the diffuser are not required.

3.1 Concept

The concept for this experiment is simple. Measurements of the solar irradiance are made from the ground before launch. Using these measurements, the initial on-orbit response of the instrument, when viewing the sun, is predicted. This requires no absolute calibration of the instrument, as was necessary for the SRBC. The experiment examines the relative change in the instrument output from the ground to orbit. This experiment hinges in large part on the quality of the atmospheric transmission measurements during the ground measurements.

The effect of the absolute value of the solar irradiance model on this experiment is very small. The instrument views the sun for both measurements, and, to an excellent approximation, the solar irradiance is removed when the ratio of the two measurements is taken.

3.2 Reflectance Equations

The transfer-to-orbit experiment uses two measurements of the sun—one from space and one from the surface of the Earth. To distinguish the two measurements, the space measurement is designated as measurement B, and the measurement from the Earth's surface as A. For the measurement from the Earth's surface, (16) is restated as

$$(DN - DN_0)_A = \frac{1}{k_2(g_A)} \frac{1}{D_A^2} \times \frac{\int_{\lambda_1}^{\lambda_2} E(S,\lambda)\, F(\lambda)\, T(\lambda)\, R(\lambda)\, d\lambda}{\int_{\lambda_1}^{\lambda_2} R(\lambda)\, d\lambda}. \quad (21)$$

where $(DN - DN_0)_A$ is the net counts from the instrument for the solar measurement from the Earth, D_A is the Earth–sun distance for the measurement, and $k_2(g_A)$ is the calibration coefficient. This equation, (21), also includes $T(\lambda)$, which is the transmittance of the atmosphere at the time of measurement from the Earth's surface. Because the atmospheric transmittance can change the radiance measured by a band by a factor of three or more, the optimum gain for the Earth-based measurement is not the same as that for the measurement from space. For the measurement from space,

$$(DN - DN_0)_B = \frac{1}{k_2(g_B)} \frac{1}{D_B^2} \times \frac{\int_{\lambda_1}^{\lambda_2} E(S,\lambda)\, F(\lambda)\, T(\lambda)\, R(\lambda)\, d\lambda}{\int_{\lambda_1}^{\lambda_2} R(\lambda)\, d\lambda}. \quad (22)$$

where $(DN - DN_0)_B$ is the net counts from the instrument for the solar measurement from space, D_B is the Earth–sun distance for the measurement, and $k_2(g_B)$ is the calibration coefficient.

In the transfer-to-orbit experiment, (21) and (22) are used to predict the net counts from the instrument for the initial view of the sun on orbit. This is done by taking the ratio of (22) to (21).

$$\frac{(DN - DN_0)_B}{(DN - DN_0)_A} = \frac{D_A^2\, k_2(g_A)}{D_B^2\, k_2(g_B)} \times \frac{\int_{\lambda_1}^{\lambda_2} E(S,\lambda)\, F(\lambda)\, R(\lambda)\, d\lambda}{\int_{\lambda_1}^{\lambda_2} E(S,\lambda)\, F(\lambda)\, T(\lambda)\, R(\lambda)\, d\lambda}. \quad (23)$$

By rearranging (23) it is possible to isolate the net counts for the measurement from space on the left side of the equation. This requires knowledge of the Earth–sun distance for the measurement on orbit. Other than that, all of the values required to predict the initial counts on orbit are known before launch.

$$(DN - DN_0)_B = (DN - DN_0)_A \frac{D_A^2\, k_2(g_A)}{D_B^2\, k_2(g_B)} \times \frac{\int_{\lambda_1}^{\lambda_2} E(S,\lambda)\, F(\lambda)\, R(\lambda)\, d\lambda}{\int_{\lambda_1}^{\lambda_2} E(S,\lambda)\, F(\lambda)\, T(\lambda)\, R(\lambda)\, d\lambda}. \quad (24)$$

The fundamental equation for the transfer-to-orbit experiment is (24). The solar irradiance spectrum of Wehrli (Sect. 5.3.2.1.) is used for the solution to this equation. The reflectance, $F(\lambda)$, is that for the SeaWiFS diffuser cover (Sect. 5.4), and the atmospheric transmittance is that in Sect. 2.3.3.

Because the calibration coefficients $k_2(g_A)$ and $k_2(g_B)$ are used in a ratio in (24), only their values relative to each other are necessary. For the solution of (24), the calibration coefficients from Table 6 are used. These coefficients are shown in Table 19. The Wehrli-based calibration coefficients cannot be used, since they are available only for the gains of the ground measurements.

In the calculations below, the integrals in the numerator and denominator of (24) are determined using summations with a step size of 1 nm. In addition, the values for the numerator and denominator are calculated as intermediate products and are shown in Table 20. The mathematical representations for the integrals are cumbersome to use in the headers of Table 20. As a result, two shorthand terms are used. The first is

$$I_G = \int_{\lambda_1}^{\lambda_2} E(S,\lambda)\, F(\lambda)\, T(\lambda)\, R(\lambda)\, d\lambda, \quad (25)$$

which is the integral in the denominator of (24), where I_G is the instrument response for the ground measurement. The second is

$$I_O = \int_{\lambda_1}^{\lambda_2} E(S,\lambda)\, F(\lambda)\, R(\lambda)\, d\lambda, \quad (26)$$

which is the integral in the numerator of (24) where I_O is the instrument response on orbit.

3.3 In-Flight Measurements

These measurements are the second of the two part process that started with the ground-based measurements on 1 November 1993.

Table 19. Calculation of the multiplier before the ratio of integrals in (24). The multiplier, listed in the final column, contains the Earth–sun distances and the calibration coefficients for the ground measurements and the initial solar measurements on-orbit. The Earth–sun distances are in astronomical units (AU). The calibration coefficients, $k_2(g)$, are taken from Table 6. They have units of $\mathrm{mW\,cm^{-2}\,sr^{-1}\,\mu m^{-1}\,count^{-1}}$. Here $R(D^2)$ is the ratio of D_A^2 to D_B^2; $R(k_2)$ is the ratio of $k_2(g_A)$ to $k_2(g_B)$; and $R(k_2D^2)$ is the ratio of $k_2(g_A)D_A^2$ to $k_2(g_B)D_B^2$.

Band	D_A	D_B	$R(D^2)$	$k_2(g_A)$	$k_2(g_B)$	$R(k_2)$	$R(k_2D^2)$
1	0.9923	1.0150	0.9558	0.007348	0.010897	0.6737	0.6439
2	0.9923	1.0150	0.9558	0.008213	0.013541	0.6060	0.5792
3	0.9923	1.0150	0.9558	0.010655	0.011842	0.8996	0.8598
4	0.9923	1.0150	0.9558	0.009189	0.011564	0.7942	0.7591
5	0.9923	1.0150	0.9558	0.007483	0.011488	0.6517	0.6228
6	0.9923	1.0150	0.9558	0.006303	0.011247	0.5606	0.5358
7	0.9923	1.0150	0.9558	0.005168	0.009332	0.5529	0.5284
8	0.9923	1.0150	0.9558	0.004221	0.007872	0.5360	0.5123

Table 20. Calculation of the predicted counts (DN) for the initial solar measurement by SeaWiFS. I_G represents the integral in the numerator of (24), and it is defined in (25). I_O represents the integral in the denominator of (24), and it is defined in (26). Both integrals have units of $\mathrm{mW\,cm^{-2}\,sr^{-1}}$. $R(k_2D^2)$ is the ratio of $k_2(g_A)D_A^2$ to $k_2(g_B)D_B^2$ from Table 19.

Band	$(DN-DN_0)_A$	$R(k_2D^2)$	I_G	I_O	I_O:I_G	$(DN-DN_0)_B$
1	195	0.6439	215.74	742.51	3.442	432.12
2	236	0.5792	474.30	1339.19	2.824	385.95
3	229	0.8598	936.10	2148.17	2.295	451.84
4	275	0.7591	1217.71	2644.36	2.172	453.31
5	358	0.6228	1322.10	2585.06	1.955	435.98
6	443	0.5358	1364.03	2165.52	1.588	376.80
7	447	0.5284	2162.61	3395.14	1.570	370.84
8	526	0.5123	2319.97	3111.32	1.341	361.40

3.3.1 Predicted Values

Tables 19 and 20 give the prelaunch prediction for the solar-based counts from the SeaWiFS bands at the start of the mission on orbit; for these calculations, that date was 1 August 1997. For this date, the Earth–sun distance was 1.0150 AU; and for the ground-based measurements, the Earth–sun distance was 0.9923 AU.

Table 19 shows the calculation of the multiplier that is before the integrals in (24). This term includes the ratio of the Earth–sun distances, as well as the ratio of the calibration coefficients. The complete multiplication term is given in the last column of Table 19. The other columns in the table are included to show the size of the individual factors in the multiplication term.

Table 20 gives the calculation of the predicted counts from SeaWiFS, $(DN-DN_0)_B$, for the first solar measurement. The ratio of integrals in the table show the contribution of atmospheric attenuation to the ground measurements. For SeaWiFS band 1 (nominal 412 nm center wavelength), atmospheric attenuation decreases the counts from the instrument by a factor of 3.4, compared to the counts at the top of the atmosphere.

3.3.2 Diffuser Changes After Launch

SeaWiFS was launched on 1 August 1997. The first solar measurements were made on day 39 after launch. The digital numbers from these measurements (DN_M) are listed in Table 21. They are also compared with the predicted counts (DN_P) from the prelaunch measurements, given as $(DN-DN_0)_B$ in Table 20. The average agreement with the predicted counts is unity at the 0.1% level, with a standard deviation of 1.4%. On day 39 after launch, regular, daily measurements of the sun were started. On day 72 there was a problem with the constants for orbit determination uplinked to the satellite, which caused the satellite computer to shut down and go into safe-haven. On day 80, regular solar measurements were restarted.

The panels in Fig. 10 show the set of solar measurements for the eight SeaWiFS bands through day 120 after launch. These measurements have been normalized to unity on day 39 to provide consistent vertical scales for the results from the eight bands. The measurements have been corrected for the Earth–sun distance. The measurements have also been corrected for the angular response of the SeaWiFS diffuser as provided in Barnes and Eplee (1996). The break in the SeaWiFS measurements at day 72 after

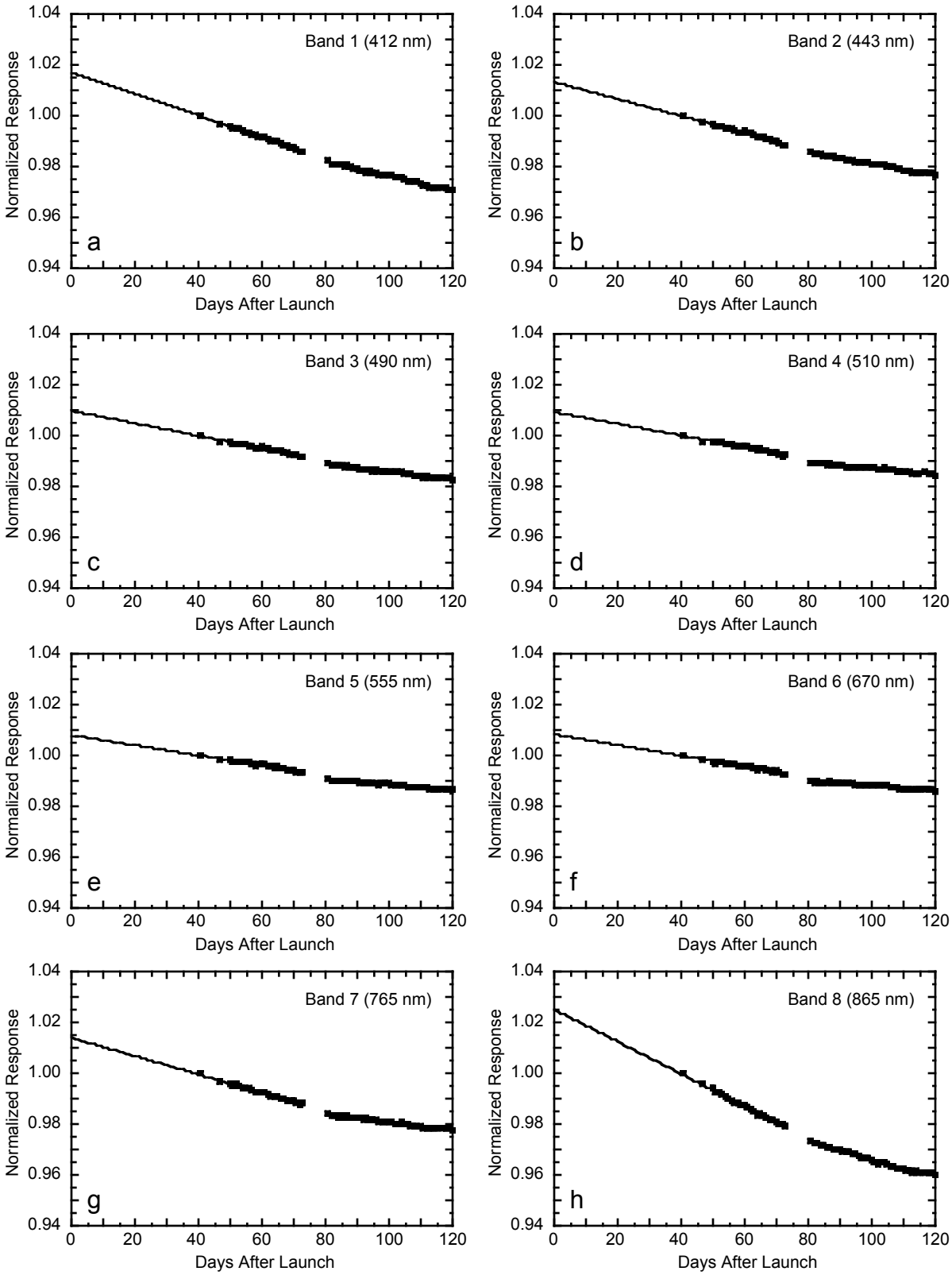

Fig. 10. Normalized diffuser radiances for the SeaWiFS bands. The data extend from day 39 after launch to day 120; the radiances are normalized to unity at day 39. The line in each panel is derived from a linear fit to the values for days 39 through 72, and there is a break in the data set from day 72 to day 80. In the panels, the symbols give the measurements, and the curves give the extrapolations to the launch date.

Table 21. Comparison of the predicted counts to the measured counts from orbit.

Band No.	DN_P	DN_M	DN_M: DN_P	Day Zero Extrapolation	DN_E	DN_E: DN_P
1	432.12	417.99	0.967	1.0172	425.18	0.984
2	385.95	385.62	0.999	1.0134	390.79	1.013
3	451.84	455.91	1.009	1.0099	460.42	1.019
4	453.31	455.99	1.006	1.0094	460.28	1.015
5	435.98	440.32	1.010	1.0081	443.89	1.018
6	376.80	378.00	1.003	1.0084	381.18	1.012
7	370.84	374.46	1.010	1.0140	379.70	1.024
8	361.40	359.62	0.995	1.0252	368.68	1.020
		Mean	1.000			1.013
		Standard Deviation	0.013			0.012

launch provided a reasonable end to the initial phase of the operation of SeaWiFS on orbit.

As shown in Fig. 10, there is no seamless transition in the solar diffuser measurements from day 72 to day 80. There are changes in the diffuser radiances during this period that are not immediately obvious from the data set. The causes for the changes are not known. For this reason, the data from day 39 to day 72 in Fig. 10 are considered the best representatives for the trend in the diffuser radiances during the initial phase of operation of the instrument on orbit. As such, they provide the best basis for an extrapolation to provide an estimate of the changes in the diffuser radiances from the first day on orbit to the first day of solar diffuser measurements.

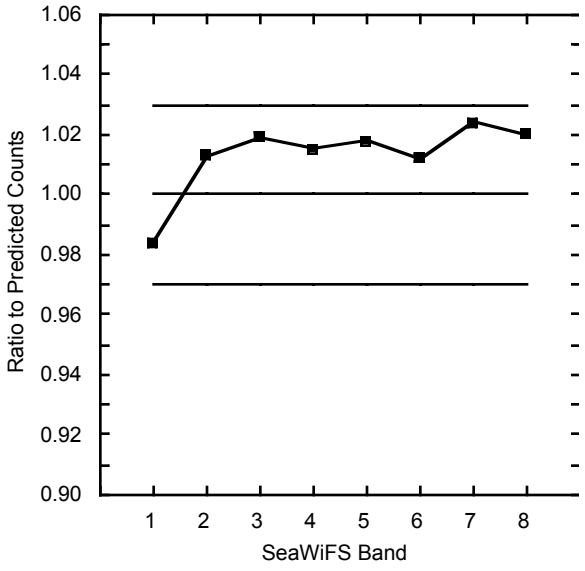

Fig. 11. The ratio of the SeaWiFS diffuser measurement calculated for day 1 on orbit relative to those predicted from the ground measurements before launch. The squares give the ratios for the eight SeaWiFS bands.

For the initial solar measurements, from day 39 to day 72, the change in the values from Fig. 10 are very close to linear with time. As a result, a linear curve fit is used for each band to estimate the change in the diffuser (in fractional terms) from the launch date to day 39. The extrapolations indicate that, if there were solar measurements on the launch date, their values would be 1–2% larger than the values on day 39. These extrapolation-based corrections of the day 39 counts are shown in Table 21. They convert the measured digital numbers (DN_M) to the extrapolated ones (DN_E).

Table 21 also shows the ratios of the DN_E to the DN_P. These ratios show the counts on orbit to average 1.2% higher than the predicted counts. Fig. 11 shows the individual ratios of the DN_E to the DN_P. The results in Fig. 11 indicate that there was no change in the sensitivity of SeaWiFS to radiant flux at the 3% level between the field measurements on 1 November 1993 and insertion into orbit on 1 August 1997.

3.4 Discussion

The results in Table 21 show the counts from the instrument on the first day on orbit (1 August 1997) to average 1.3% higher than predicted with a standard deviation of 1.2%. The greatest relative difference from the predicted counts is 2.4% for band 7. The results in Table 21 include a correction for changes in the reflectance of the diffuser for the period between the launch of the instrument and the date of the first solar measurement—39 days later on 9 September 1997.

There are three uncertainties in the transfer-to-orbit experiment. The first is the uncertainty in the atmospheric correction, which as in the SRBC, is about 3% (Biggar et al. 1993a, 1993b, and 1999). The second is the uncertainty in the reflectance of the diffuser for the two parts of the experiment. This does not arise from the absolute value for the reflectance, but from the uncertainty in the alignment of the diffuser during the ground portion of the experiment (Sect. 2.3.4.3). The authors estimate this uncertainty at about 0.4% (Biggar et al. 1999). It represents a difference of about one-fourth of a degree in the angle of the solar flux from the normal to the input aperture of the diffuser

housing (Biggar et al. 1999). The third uncertainty arises from the changes in the reflectance of the diffuser from the launch of SeaWiFS to the date of the first measurements of the sun. The corrections for these changes are about 1–2%. Because an extrapolation is required for these corrections, the authors estimate the uncertainty in this factor to be about 1%. For the three uncertainties, the square root of the sum of the squares is about 3 or 4%.

Editorial Note

This document is presented *as submitted* with minor modifications to correct typographical or obvious clerical errors and to maintain the established style of the *SeaWiFS Postlaunch Technical Report Series*.

Glossary

`6S`	Not an acronym, but an atmospheric photochemical and radiative transfer model.
AU	Astronomical Unit
BRDF	Bidirectional Reflectance Distribution Function
FEL	Not an acronym, but a type of lamp designator.
GSFC	Goddard Space Flight Center
`MODTRAN`	Not an acronym, but an atmospheric photochemical and radiative transfer model.
NASA	National Aeronautics and Space Admininstation
PST	Pacific Standard Time
RSR	Relative Spectral Response
SeaWiFS	Sea-viewing Wide Field-of-view Sensor
SBRC	Raytheon Santa Barbara Research Center (formerly Hughes Santa Barbara Research Center)
SBUV	Solar Backscatter Ultraviolet Radiometer
SRBC	Solar Radiation-Based Calibration
YB71	Not an acronym, but a type of paint for solar diffusers.

Symbols

A_I	Incidence area on the scattering surface.
A_S	Scattering area on the scattering surface.
a_0	The polynomial coefficient for the BRDF wavelength dependence.
a_1	The polynomial coefficient for the BRDF wavelength dependence.
$B(\lambda)$	Bidirectional reflectance distribution function.
D	Earth-sun distance.
D_A	Earth-sun distance for the ground measurements.
D_B	Earth-sun distance for the on-orbit measurements.
DN	Digital number.
$(DN-DN_0)_A$	Net counts from the instrument for the solar measurement from the Earth.
$(DN-DN_0)_B$	Net counts from the instrument for the solar measurement from space.
DN_E	Net digital numbers extrapolated for measurements on-orbit.
DN_M	Net digital numbers measured on-orbit.
DN_P	Net digital numbers predicted for measurements on-orbit.
DN_0	Digital number with no input radiance.
$d\Omega$	Differential of solid angle.
$E(S,\lambda)$	Solar spectral irradiance.
$E(\lambda)$	Spectral irradiance.
$E(\lambda)\theta_I$	Incident irradiance.
E_B	Band-averaged spectral irradiance.
$F(\lambda)$	Bidirectional reflectance distribution function (simplified for SeaWiFS measuring conditions).
F_B	Band-averaged BRDF.
g	SeaWiFS gain factor.
g_A	Gain for the ground measurements.
g_B	Gain for the on-orbit measurements.
g_1	Gain for channel 1.
g_2	Gain for channel 2.
g_3	Gain for channel 3.
g_4	Gain for channel 4.
I_G	Integral in the denominator of (24).
I_O	Integral in the numerator of (24).
$k_2(g)$	SeaWiFS calibration coefficient.
$k_2(g_A)$	Calibration coefficient for ground measurements.
$k_2(g_B)$	Calibration coefficient for on-orbit measurements.
$\overline{L}$	Band-averaged spectral radiance.
$L(\lambda)$	Spectral radiance.
$L(\lambda)\theta_S$	Scattered radiance at wavelength λ.
$\overline{L}_G(\lambda)$	Band-averaged spectral radiance for the ground measurement.
$Q(\lambda)$	Quantum efficiency.
$R(D^2)$	Ratio of D_A^2 to D_B^2.
$R(k_2)$	Ratio of $k_2(g_A)$ to $k_2(g_B)$.
$R(k_2D^2)$	Ratio of $k_2(g_A)D_A^2$ to $k_2(g_B)D_B^2$.
$R(\lambda)$	Spectral response.
$T(\lambda)$	Atmospheric transmittance.
T_B	Band-averaged atmospheric transmittance.
λ	Wavelength dependence of the reflectance.
ξ	Reflecting-transmitting efficiency of the optical components.
θ_I	Incidence angle
θ_S	Scattering angle.
λ	Wavelength.
λ_B	Band-averaged center wavelength for a source with a constant spectral radiance of unity.
λ_1	Lower limits of integration.
λ_2	Upper limits of integration.

References

Barnes, R.A., 1994: *SeaWiFS Data: Actual and Simulated.* [World Wide Web page.] From URLs: `http://seawifs.gsfc.nasa.gov/SEAWIFS/IMAGES/spectra1.dat` and `/spectra2.dat` NASA Goddard Space Flight Center, Greenbelt, Maryland.

——, 1996: "SeaWiFS center wavelengths." In: SeaWiFS Calibration Topics, Part 1. *NASA Tech. Memo. 104566, Vol. 39,* S.B. Hooker and E.R. Firestone Eds., NASA Goddard Space Flight Center, Greenbelt, Maryland, 49–53.

——, 1997: "SeaWiFS measurements in orbit: Band-averaged spectral radiance." In: SeaWiFS Calibration Topics, Part 2. *NASA Tech. Memo. 104566, Vol. 40*, S.B. Hooker and E.R. Firestone Eds., NASA Goddard Space Flight Center, Greenbelt, Maryland, 48–55.

——, and R.E. Eplee, Jr., 1996: "The SeaWiFS solar diffuser." In: SeaWiFS Calibration Topics, Part 1. *NASA Tech. Memo. 104566, Vol. 39,* S.B. Hooker and E.R. Firestone Eds., NASA Goddard Space Flight Center, Greenbelt, Maryland, 54–61.

——, and ——, 1997: "The 1993 SeaWiFS calibration using band-averaged spectral radiances." In: SeaWiFS Calibration Topics, Part 2. *NASA Tech. Memo. 104566, Vol. 40,* S.B. Hooker and E.R. Firestone Eds., NASA Goddard Space Flight Center, Greenbelt, Maryland, 39–47.

——, and W.E. Esaias, 1997: "A nominal top-of-the-atmosphere spectrum for SeaWiFS." In: SeaWiFS Calibration Topics, Part 2. *NASA Tech. Memo. 104566, Vol. 40,* S.B. Hooker and E.R. Firestone Eds., NASA Goddard Space Flight Center, Greenbelt, Maryland, 3–11.

——, A.W. Holmes, W.L. Barnes, W.E. Esaias, C.R. McClain, and T. Svitek, 1994: SeaWiFS Prelaunch Radiometric Calibration and Spectral Characterization. *NASA Tech. Memo. 104566, Vol. 23,* S.B. Hooker, E.R. Firestone, and J.G. Acker, Eds., NASA Goddard Space Flight Center, Greenbelt, Maryland, 55 pp.

——, R.E. Eplee, Jr., F.S. Patt, and C.R. McClain, 1999: Changes in the radiometric sensitivity of SeaWiFS. *Appl. Opt.,* (in press).

Berk, A., L.S. Bernstein, and D.C. Robertson, 1989: `MODTRAN`: A moderate resolution model for `LOWTRAN7`. *Tech. Report GL-TR-90-0122,* Geophysical Directorate Phillips Laboratory, Hanscom AFB, Massachusetts, 44 pp.

Biggar, S.F., D.I. Gelman, and P.N. Slater, 1990: Improved evaluation of optical depth components from Langley plot data. *Remote Sens. Environ.,* **32,** 91–101.

——, K.J. Thome, P.N. Slater, A.W. Holmes, and R.A. Barnes, 1993a: Preflight solar radiation-based calibration of SeaWiFS. *SPIE,* **1939,** 233–242.

——, K.J. Thome, P.N. Slater, A.W. Holmes, and R.A. Barnes, 1993b: "Preflight solar radiation-based calibration of SeaWiFS." In: Case Studies for SeaWiFS Calibration and Validation, Part 2. *NASA Tech. Memo. 104566, Vol. 19,* S.B. Hooker, E.R. Firestone, and J.G. Acker, Eds., NASA Goddard Space Flight Center, Greenbelt, Maryland, 25–32.

——, K.J. Thome, P.N. Slater, A.W. Holmes, and R.A. Barnes, 1995: "Second SeaWiFS preflight solar radiation-based calibration experiment." In: Case Studies for SeaWiFS Calibration and Validation, Part 3. *NASA Tech. Memo. 104566, Vol. 27,* S.B. Hooker, E.R. Firestone, and J.G. Acker, Eds., NASA Goddard Space Flight Center, Greenbelt, Maryland, 20–24.

——, P.N. Slater, J.M. Palmer, and K.J. Thome, 1999: Unified approach to absolute radiometric calibration in the solar-reflective range. *Remote Sens. Environ.,* (accepted).

Bruegge, C.J., V.G. Duval, N.L. Chrien, and D.J. Diner, 1993: Calibration plans for the multi-angle, imaging spectroradiometer (MISR). *Metrologia,* **30,** 231–221.

Flittner, D.E., and P.N. Slater, 1991: Stability of narrow-band filter radiometers in the solar-reflected range. *Photogramm. Eng. Remote Sens.,* **57,** 165–171.

Gordon, H.R., 1995: Remote sensing of ocean color: A methodology for dealing with broad spectral bands and significant out-of-band response. *Appl. Opt.,* **34,** 8,363–8,374.

Johnson, B.C., S.S. Bruce, E.A. Early, J.M. Houston, T.R. O'Brian, A. Thompson, S.B. Hooker, and J.L. Mueller, 1996: The Fourth SeaWiFS Intercalibration Round Robin Experiment (SIRREX-4), May 1995. *NASA Tech. Memo. 104566, Vol. 37,* S.B. Hooker and E.R. Firestone, Eds., NASA Goddard Space Flight Center, Greenbelt, Maryland, 65 pp.

——, F. Sakuma, J.J. Butler, S.F. Biggar, J.W. Cooper, J. Ishida, and K. Suzuki, 1997: Radiometric measurement comparison using the Ocean Color Temperature Scanner (OCTS) visible and near infrared integrating sphere. *J. Res. Natl. Inst. Stand. Technol.,* **102,** 627–646.

——, E.A. Early, R.E. Eplee, Jr., R.A. Barnes, and R.T. Caffrey, 1999: The 1997 Prelaunch Calibration of SeaWiFS. *NASA Tech. Memo. 1999–206892, Vol. 4,* S.B. Hooker and E.R. Firestone, Eds., NASA Goddard Space Flight Center, Greenbelt, Maryland, 51 pp.

Lang, K.R., 1980: *Astrophysical Formulae,* Second Edition, Springer-Verlag, New York, 783 pp.

Neckel, H., and D. Labs, 1984: The solar radiation between 3,300 and 12,500Å. *Solar Physics,* **90,** 205–258.

Pagano, T.S., and R.M. Durham, 1993: Moderate Resolution Imaging Spectroradiometer (MODIS). *SPIE,* **1939,** 2–17.

Slater, P.N., and J.M. Palmer, 1991: Solar-diffuser panel and ratioing radiometer approach to satellite sensor on-board calibration. *SPIE,* **1493,** 100–105.

Smith, E.V.P., and D.M. Gottlieb, 1974: Solar flux and its variation. *Space Sci. Rev.,* **16,** 771–802.

Thuillier, G., M. Herse, P.C. Simon, D. Labs, H. Mandel, and D. Gillotay, 1998: Observation of the solar spectral irradiance from 200 to 870 nm during the ATLAS 1 and 2 missions by the SOLSPEC spectrometer. *Metrologia,* **35,** 689–695.

Vermote, E.F., D. Tanre, J.L. Deuze, M. Herman, and J-J. Morcrette, 1997: Second simulation of the satellite signal in the solar spectrum, `6S`: An Overview. *IEEE Trans. Geosci. Remote Sens.,* **35,** 675–686.

Wehrli, C., 1985: *Extraterrestrial Solar Spectrum,* Publ. 615, *Physikalisch-Meterologisches Observatorium* Davos and World Radiation Center, Davos-Dorf, Switzerland, 23 pp.

The SeaWiFS Postlaunch Technical Report Series

Vol. 1

Johnson, B.C., J.B. Fowler, and C.L. Cromer, 1998: The SeaWiFS Transfer Radiometer (SXR). *NASA Tech. Memo. 1998–206892, Vol. 1,* S.B. Hooker and E.R. Firestone, Eds., NASA Goddard Space Flight Center, Greenbelt, Maryland, 58 pp.

Vol. 2

Aiken, J., D.G. Cummings, S.W. Gibb, N.W. Rees, R. Woodd-Walker, E.M.S. Woodward, J. Woolfenden, S.B. Hooker, J-F. Berthon, C.D. Dempsey, D.J. Suggett, P. Wood, C. Donlon, N. González-Benítez, I. Huskin, M. Quevedo, R. Barciela-Fernandez, C. de Vargas, and C. McKee, 1998: AMT-5 Cruise Report. *NASA Tech. Memo. 1998–206892, Vol. 2,* S.B. Hooker and E.R. Firestone, Eds., NASA Goddard Space Flight Center, Greenbelt, Maryland, 113 pp.

Vol. 3

Hooker, S.B., G. Zibordi, G. Lazin, and S. McLean, 1999: The SeaBOARR-98 Field Campaign. *NASA Tech. Memo. 1999–206892, Vol. 3,* S.B. Hooker and E.R. Firestone, Eds., NASA Goddard Space Flight Center, Greenbelt, Maryland, 40 pp.

Vol. 4

Johnson, B.C., R.E. Eplee, Jr., R.A. Barnes, E.A. Early, and R.T. Caffrey, 1999: The 1997 Prelaunch Radiometric Calibration of SeaWiFS. *NASA Tech. Memo. 1999–206892, Vol. 4,* S.B. Hooker and E.R. Firestone, Eds., NASA Goddard Space Flight Center, Greenbelt, Maryland, 51 pp.

Vol. 5

Barnes, R.A., R.E. Eplee, Jr., S.F. Biggar, K.J. Thome, E.F. Zalewski, P.N. Slater, and A.W. Holmes 1999: The SeaWiFS Solar Radiation-Based Calibration and the Transfer-to-Orbit Experiment. *NASA Tech. Memo. 1999–206892, Vol. 5,* S.B. Hooker and E.R. Firestone, Eds., NASA Goddard Space Flight Center, 28 pp.